General Disclaimer

One or more of the Following Statements may affect this Document

- This document has been reproduced from the best copy furnished by the organizational source. It is being released in the interest of making available as much information as possible.

- This document may contain data, which exceeds the sheet parameters. It was furnished in this condition by the organizational source and is the best copy available.

- This document may contain tone-on-tone or color graphs, charts and/or pictures, which have been reproduced in black and white.

- This document is paginated as submitted by the original source.

- Portions of this document are not fully legible due to the historical nature of some of the material. However, it is the best reproduction available from the original submission.

Contract Number: NAS9-15212

DRL Number: T-1349

Line Item Number: 3

DRD Number: MA-183TA

CR 151821

FINAL REPORT

EXHIBIT B
STATEMENT OF WORK

IONOSPHERE/MICROWAVE BEAM INTERACTION STUDY

Prepared for

NATIONAL AERONAUTICS AND SPACE ADMINISTRATION
LYNDON B. JOHNSON SPACE CENTER

Prepared by

Wm. E. Gordon and Lewis M. Duncan

WILLIAM MARSH RICE UNIVERSITY
Houston, Texas

July 1978

Contract Number: NAS9-15212
DRL Number: T-1349
Line Item Number: 3
DRD Number: MA-183TA

FINAL REPORT

EXHIBIT B
STATEMENT OF WORK

IONOSPHERE/MICROWAVE BEAM INTERACTION STUDY

Prepared for

NATIONAL AERONAUTICS AND SPACE ADMINISTRATION
LYNDON B. JOHNSON SPACE CENTER

Prepared by

Wm. E. Gordon and Lewis M. Duncan

WILLIAM MARSH RICE UNIVERSITY
Houston, Texas

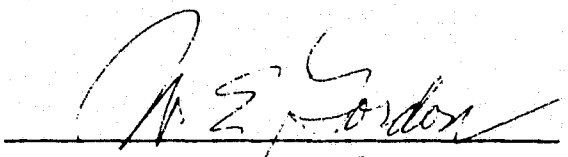

Wm. E. Gordon
Principal Investigator

July 1978

ABSTRACT

IONOSPHERE/MICROWAVE BEAM INTERACTION STUDY

The microwave beam of the Solar Power Satellite (SPS) is predicted to interact with the ionosphere producing thermal runaway up to an altitude of about 100 kilometers at a power density threshold of 12 mW/cm^2 (within a factor of two). The previous study reaffirmed the predicted threshold for thermal self-focusing at a power density of 20 mW/cm^2 (within a factor of two). Neither of these predictions have been verified by experiment, although tests have been proposed.

The operation of the SPS at two frequencies, 2450 and 5800 MHz, is compared. The ionospheric interaction is less at the higher frequency, but the tropospheric problem (scattering from heavy rain and hail) is worse at the higher frequency. A meaningful comparison requires a common yardstick such as the cost in dollars associated with each effect. The cost of correcting any communication problems that might arise cannot be estimated until the problems are defined by experiment. The cost of power lost through rain and hail could be estimated for particular receiving sites given the expected kilowatt-hour charge.

The SPS microwave beam will be formed and directed by phase information derived from a pilot signal transmitted from the ground and received in a number of module locations on the SPS antenna. Inasmuch as microwave signals from communication satellites have been observed to scintillate, there is some concern that the uplink pilot signal may be distorted by the SPS heated ionosphere. The microwave scintillations are only observed in the tropics in the early evenings near the equinoxes, apparently when the ionosphere is disturbed. These observations have not yet been satisfactorily explained and, therefore, considerable doubt is

cast on any calculated pilot beam effects. While the calculated phase fluctuations are small, they should not be used until they can be verified by an experiment.

An extension of the experiment simulating SPS microwave beam/ionosphere interaction proposed in the previous report on this contract is suggested. The extension to the test provides for receiving microwave communication signals from geosynchronous satellites through the ionosphere disturbed by the ground transmitter. This transmitter heats the ionosphere at the same rate and over the same volume as the SPS microwave would. The phase and amplitude fluctuations and their correlation distances in two directions measured on the ground provide the information needed to evaluate the uplink signal performance.

If the test indicates large phase errors in the uplink pilot signal there are ways of reducing the effects and two of these are outlined.

TABLE OF CONTENTS

CHAPTER 1

RESULTS

1.1 Non-linear Interactions

Ohmic heating of the ionosphere continues to be the driving force for instabilities in the plasma and the heating is inversely proportional to the square of the frequency (see Section 3.1). Thermal runaway is predicted within a factor of two to occur at a power density of 12 mW/cm^2 for the 2.45 GHz SPS frequency (see Section 3.2). The theory and observations of thermal self-focusing are in agreement when the ionospheric plasma is overdense (the local plasma frequency exceeds the heating frequency). However, there are no observations available to compare with the theory of thermal self-focusing for the SPS case, underdense ionospheric plasma (the local plasma frequency is less than the heating frequency), and these observations, supplemented by full diagnostics, are needed to verify the frequency and power density scaling relationships. The calculated limiting angles for the formation of striations are smaller for higher beam frequencies, restricting the communication effects, if any, of thermal self-focusing even more severely (see Section 3.3).

1.2 Comparison of SPS Operation on 2450 and 5800 MHz

The microwave/ionosphere interactions are less severe at the higher frequency. The effects driven by ohmic heating will be less because the ohmic heating is inversely proportional to the frequency squared (see Section 4.1).

The microwave/neutral atmosphere interactions are slightly more severe at the higher frequency, but the effects are about 2 percent at both frequencies (see Sections 4.2 and 4.5).

The microwave attenuation by hydrometers (rain, snow and hail) are more severe at the higher frequency. Half or more of the SPS power at either frequency may be lost to the rectenna through a hailstorm with large, wet stones. The outage from heavy hailstorms varies across the country, but is likely to be a few occurrences per year each of duration five to ten minutes (see Section 4.4).

The choice of frequency, aside from the political and frequency allocation aspects, depends on a common scale of values applied to the ionospheric and tropospheric impacts. The ionospheric effects argue for a higher frequency, but the cost in dollars, say, of the solutions to the communication problems that may arise is not available until after the simulated SPS tests are conducted and evaluated. The tropospheric effects lead to loss of power from the SPS beam and the magnitude and expected durations of these losses can be estimated and assigned a dollar value for rectennas located in particular areas of the country. From these a cost-effectiveness for each frequency could be established (see Section 4.5). In the meantime, a clear choice cannot be made.

1.3 Perturbations of the Uplink Pilot Signal

Microwave signals propagating through the ionosphere are observed to scintillate at certain times (evenings around the equinoxes) in the tropics contrary to theoretical predictions (see Section 5.2). Similar scintillations have been observed through aurora. Neither of these will affect mid-latitude consumers, but the tropical observations would be a factor if the SPS is to supply users at latitudes below about 20 degrees.

Although a few claims have been made, there is no satisfactory explanation of the observed scintillations. This condition may be changing (see Sections 5.3 and 5.4).

The failure of theory to explain observed microwave scintillation through the ionosphere and the present stage of development of the theory of microwave modification of the ionospheric plasma make it impossible to predict the effects of an ionosphere heated by the SPS beam on the uplink pilot beam (see Section 5.5). The effects can be measured in an extension of the proposed simulated SPS experiment.

If the uplink is disturbed by the SPS heated ionosphere the effects can be mitigated by averaging the phase information over time and/or by moving the pilot transmitter away from the rectenna (see Section 5.6).

The uplink and the SPS frequencies must be separated sufficiently that the interaction of the two frequencies in the ionospheric plasma does not excite instabilities (see Section 5.1).

CHAPTER 2

RECOMMENDATIONS

2.1 An HF heater should be designed, built and operated to reproduce and exceed the radio wave heating of the ionosphere by the 5 GW SPS system. The heater beam should be tiltable toward the geosynchronous orbit so that microwave signals (1.5-6 GHz) transmitted by communication satellites can be received through the disturbed ionosphere. The phase and amplitude fluctuations and the correlation distances on the ground in the north-south and east-west directions should be measured so that the corresponding ionospheric scales can be deduced and the uplink perturbations calculated.

2.2 The heating effects should be mapped and measured by an incoherent scatter radar, by photometers and by ionosondes so that the scaling from HF to S-band can be made with confidence. These diagnostics must be used for the understanding of both the ionospheric instabilities, if any, and for the uplink perturbations, if any.

2.3 The dollar costs of solving any communication problems that arise from the SPS operating at 2450 and 5800 MHz, as indicated by the proposed tests, should be compared with the dollar income lost when the SPS beam traverses rain and hail for typical receiving sites. The comparison should be a factor along with political considerations related to frequency allocations in selecting the SPS operating frequency.

2.4 Theoretical and experimental investigations should be continued into the physics of nonlinear wave-plasma interactions, plasma turbulence, and the ionospheric processes associated with substantial local heating. Interim tests using available facilities are underway and should be continued pending the availability of the full-scale simulation of the SPS microwave beam/ionosphere interaction.

2.5 The frequencies transmitted by the uplink pilot and by the SPS must be separated sufficiently so that the frequency difference does not act to pump the ionospheric plasma and produce instabilities. The separation should be more than twice the highest plasma frequency expected for the local ionosphere.

CHAPTER 3

IONOSPHERE/MICROWAVE INTERACTIONS

Task: Document an analysis which continues the studies determining the power density levels at which nonlinear microwave/ionospheric interactions begin to occur.

The study of ionosphere/microwave interactions is motivated by its application to the design and environmental impact assessment of a solar power satellite (SPS). After collecting solar energy in space, the SPS will microwave beam energy to a ground-based rectenna site, where it can be converted directly into electricity. Microwave interactions with the ionosphere critically affect the design and impact of this microwave power transmission system.

Heating of the ionosphere by the microwave beam may generate ionospheric conditions leading to communications, navigation and radar systems interference, as well as producing potential climatic effects. Disturbed ionospheric conditions accompanying these interactions may adversely affect the microwave beam pointing system by causing scintillations in the uplink pilot beam of the active retrodirective array (see Chapter 5). In addition, the interaction thresholds impact the microwave beam power density (see Chapter 4), directly affecting the SPS economics.

Several potential ionosphere/microwave interactions have been identified and theoretically studied (Duncan and Gordon, 1977; Duncan and Zinn, 1978). These include parametric instability excitation, electron thermal runaway in the lower ionosphere, and thermal self-focusing of the microwave beam in the ionospheric F-region. Study of these phenomena is proceeding, while the search for additional interactive mechanisms continues.

A fundamental objective in our investigation of interaction processes is to establish the dependence of the interactive mechanism on parameters of the microwave beam and local ionospheric conditions. This knowledge contributes to the development of methods for avoiding or suppressing the interactions, or mitigating their effects. Because the frequency and power density of the SPS microwave beam has not been definitely established, and because high-frequency (HF) scaled experiments are proposed for the future, understanding the frequency scaling of the interactive mechanisms is a critical part of this interaction study. The following chapter describes the frequency dependence of potential interactions currently being investigated.

3.1 Ohmic Heating

Microwave radiation propagating through the ionosphere is collisionally damped by free electrons. Although the fraction of wave energy absorbed by the plasma is expected to be small, because this absorbed energy goes directly into the free electrons, whose effective heat capacity is very small, the resulting ohmic heating can significantly affect the local ionospheric thermal budget. The rate of energy input Q to the ionospheric plasma from ohmic heating is given by

$$Q = \frac{E^2}{8\pi} \frac{f_p^2}{f_o^2} (\nu_{ei} + \nu_{en}) \qquad (1)$$

$$\simeq 2.7 \times 10^{-3} (F/f_o^2)\, n_e (\nu_{ei} + \nu_{en}) \quad \text{erg/cm}^3\cdot\text{s} \qquad (2)$$

where E is the local electric field amplitude, f_p is the plasma frequency, f_o is the wave frequency, ν_{ei} and ν_{en} are the electron-ion and electron-neutral collision frequencies (sec^{-1}), n_e is the electron number density (cm^{-3}), and F is the radiation flux density ($erg/cm^3 \cdot s$). The collision frequency is approximately given by (Banks and Kockarts, 1973)

$$\nu_{en} \simeq 2.3 \times 10^{-11} n(M) T_e \quad sec^{-1} \tag{3}$$

where n(M) is the total molecular number density (cm^{-3}) and T_e is the electron temperature. Electron-neutral collisions typically dominate over electron-ion collisions in the ionosphere. Because the collision frequencies are functions of temperature, they must be self-consistently determined in any reasonable heating theory.

As shown in equation (1), ohmic heating scales as the inverse square of frequency. This relationship derives directly from the volumetric ohm's law, and thus is understood with considerable certainty. Ohmic heating of the ionospheric plasma and the resultant thermal forces may drive secondary phenomena such as an electron thermal runaway or thermal self-focusing of the microwave beam. These interactions do not necessarily scale linearly with their driving force (ohmic heating) and may occur on microscopic or macroscopic plasma scale sizes.

All of the SPS ionosphere/microwave interactions currently thought to be important are at least initially driven by ohmic heating. As a result, even though a ground-based SPS-equivalent microwave research facility is economically not feasible, definitive ground-based experiments can be designed, scaled to lower frequencies and thus requiring much smaller radiated powers in order to produce ohmic heating equivalent to that predicted for the SPS

microwave beam. The environmental impact of the ionosphere/microwave interactions, including the communications, navigation, and radar interference effects, thus could be studied directly. A detailed investigation of the interactive mechanisms using comprehensive ionospheric diagnostics would be imperative in order to establish the frequency scaling of the interactions, so that results of the scaled experiments could be extrapolated to the SPS microwave system. A preliminary analysis of the requirements for frequency-scaled experiments using the Arecibo HF ionospheric heating facility has been reported previously (Duncan and Gordon, 1977).

Changes in the SPS microwave operating frequency can significantly affect the ionospheric ohmic heating of the beam which, as noted, scales as the inverse square of frequency. Therefore, the ohmic heating produced by an SPS microwave beam operating at 2.45 GHz with a power flux of 20 mW/cm^2 is equivalent to the heating expected for a beam operating at 5.8 GHz and a power flux of approximately 112 mW/cm^2 (see Chapter 4).

3.2 Electron Thermal Runaway

Ohmic heating of the lower ionosphere by the SPS microwave beam increases the local electron kinetic temperature, which in turn increases the electron-neutral collision frequency but decreases the electron cooling rate. As a result, sufficiently strong ohmic heating can produce a continuously increasing (or runaway) electron temperature, saturating only at some level where the increased ohmic heating is balanced by additional cooling processes.

Electrons lose energy primarily through collisions with atoms and molecules of the background neutral gas. In the collision dominated lower ionosphere thermal conduction does not contribute significantly to electron cooling.

The most effective kinds of electron energy transfer collisions are inelastic interactions with O_2 and N_2, producing rotational and vibrational excitation, and collisions with atomic oxygen, producing excitation of hyperfine levels of the ^3p ground state. Computations of ionospheric electron heating within the SPS microwave beam, using a comprehensive model of the dominant collisional cooling mechanisms, predict order of magnitude increases in the electron temperature within the lower ionosphere (Duncan and Zinn, 1978; Perkins and Roble, 1978). Steady-state solutions of the electron energy equation forecast increases in the ambient electron temperature (typically $\sim$ 200°K) to a saturated temperature of approximately 2000°K.

The environmental impacts of an electron thermal runaway are unknown. An increase in the electron temperature in the lower ionosphere does not explicitly imply significant communications-related effects. The principal effect of heating the electrons is to increase radio wave absorption. Temperature-dependent ionospheric chemistry will result in a modification of the local plasma density, but probably not with a magnitude sufficient to cause any major restructuring of the ionosphere. Although collisions may prevent the formation of field-aligned irregularities, plasma striations in the E-region are a potential source of serious communications effects. In addition, strong local plasma heating frequently results in plasma turbulence, which contributes to scintillations of ground-to-satellite signals, including the uplink pilot beam.

The action of supplementary cooling processes will enhance airglow emissions, while the strong thermal forces in the plasma may excite some heretofore unrecognized secondary interactions, generating additional environmental effects. Although several independent theories (Duncan and Zinn, 1978; Perkins and Roble, 1978; Holway and Meltz, 1973)

describing the thermal runaway instability have yielded similar results, no experimental observations of electron thermal runaway in the ionosphere have been reported.

Threshold of the electron thermal runaway instability can be estimated by solving a simplified version of the electron energy equation,

$$\frac{3}{2} n_e \frac{dT_e}{dt} = Q^+ - Q^- \quad , \tag{4}$$

where n_e is the electron number density, dT_e/dt is the rate of change of the electron temperature, Q^+ is the heat source function, and Q^- describes the volume heat losses.

We consider the energy input to come entirely from ohmic heating, and the principal heat loss mechanism to be electron-rotational excitation of N_2 and O_2. Thus we are neglecting the solar heat source term and losses due to vibrational excitation of N_2 and O_2, $O(^3p)$ oxygen fine structure excitation, and thermal conduction. Vibrational excitation of N_2 becomes an important cooling process only after the electron temperature reaches $\sim$ 1500°K, and thus is not expected to contribute significantly to the threshold calculation. Similarly, below 150 km thermal conduction does not contribute to electron cooling. However, excitation of hyperfine levels of $O(^3p)$ will contribute to the determination of instability threshold, particularly at the higher altitudes. As a result, our calculated thresholds will underestimate the true threshold predictions established through sophisticated numerical computations including a detailed model ionosphere. Nevertheless, our calculation does yield a threshold value which is probably accurate to within a factor of 2, about the same accuracy to which the cooling reaction rates are known.

The heat input function Q^+ can be estimated by combining equations (2) and (3) to yield

$$Q^+ = 6.2\times10^{-14}(F/f^2)[n(N_2) + n(O_2)]n_eT_e \quad (5)$$

$$\simeq 7.4\times10^{-14}(F/f^2)n(N_2)n_eT_e \quad \text{erg/cm}^3\cdot\text{s} \quad (6)$$

where we have estimated $n(O_2)\,n(N_2) \simeq 0.2$. The heat loss function Q^- is approximated by

$$Q^- \simeq 3.2\times10^{-26}n_e(T_e - T_n)[n(N_2) + 3.5\,n(O_2)]/T_e^{1/2} \quad \text{erg/cm}^3\cdot\text{s} \quad (7)$$

$$\simeq 5.4\times10^{-26}n_e n(N_2)\,T_e^{-1/2}(T_e - T_n) \quad \text{erg/cm}^3\cdot\text{s} \quad (8)$$

where $n(N_2)$ and $n(O_2)$ are the number density of N_2 and O_2, respectively, and T_n is the neutral temperature.

The electron energy is stable wherever Q^- is greater than Q^+. Electron heating occurs when Q^+ exceeds Q^-, and the heating is unstable leading to a thermal runaway if Q^+ is greater than Q^- for all values of the heated electron temperature. Substituting equations (6) and (8) into equation (4) and solving yields the threshold condition,

$$F_{threshold} \simeq 2.8\times10^{-13}f_o^{\,2}T_n^{-1/2} \quad (9)$$

Letting f_o = 2.45 GHz and T_n = 200°K, the thermal runaway threshold for the SPS microwave beam can be estimated as $F = 1.2\times10^5$ erg/cm^2·s = 12 mW/cm^2. The corresponding threshold for f_o = 5.8 GHz is approximately F = 67 mW/cm^2.

This value is by no means an exact solution for the thermal runaway instability threshold. There is considerable uncertainty in the cooling reaction rate coefficients. Rather than use a model ionosphere, and therefore obtain threshold as a function of altitude, we have assumed typical values for ionospheric parameters at ~ 100 km when necessary for the computations. Including a model ionosphere, thermal runaway threshold increases slightly with increasing altitude. In addition, by neglecting $O(^3p)$ fine structure excitation, we have underestimated the instability threshold, with the amount of error again becoming larger with increasing altitude. Nevertheless, this calculation yields an analytic solution for thermal runaway threshold in the lower ionosphere, with an accuracy of about a factor of 2. Such a solution is valuable because it explicitly describes the electron thermal runaway threshold as a function of SPS microwave operating frequency and beam power density.

3.3 Thermal Self-Focusing

The theory of thermal self-focusing of electromagnetic waves in plasmas is developed in detail by Perkins and Valeo (1974) for both overdense and underdense heating. There are qualitative differences in the theory for overdense and underdense heating. Overdense heating corresponds to the case of heating with a frequency less than the critical frequency of the ionosphere, which is typically ~ 8 MHz in the daytime, so that the heating wave is reflected in the ionosphere. Several experiments have accomplished this type of heating in the past. Underdense heating corresponds to the case of heating with a frequency greater than the critical frequency, so that the heating wave penetrates the ionosphere. If the SPS microwave beam produces heating in the ionosphere, it will be underdense heating.

Before discussing thermal self-focusing, let us first mention some of the equivalent terminologies which can be found in the literature. Thermal self-focusing has also been referred to as thermally-driven stimulated Brillouin scattering (Fejer, 1978) in ionospheric modification theories. In nonlinear optics it is called stimulated Rayleigh scattering. As applied to laser technology, this phenomenon is described as beam filamentation. The effect of the self-focusing instability, which we call irregularities or plasma striations, is frequently referred to as "hot spots" in laser-plasma coupling, as well as "solitons" in astrophysical and controlled fusion research. Nevertheless, the physics of self-focusing is essentially the same for each of these applications.

The physical picture of thermal self-focusing can be understood by considering the following plasma model, which is illustrated in Figure 3.1. Small natural density fluctuations cause a variation in the plasma's index of refraction. The incident wave focuses and defocuses as it passes through these fluctuations. In regions where the plasma is relatively less dense, the electric field intensity of the wave is increased slightly. This increased electric field intensity causes more plasma to drift out of the less dense regions because of ohmic heating or the electric field ponderomotive force. Thus the initial perturbation is amplified. This self-focusing instability continues until hydrodynamic equilibrium is reached, creating large scale irregularities aligned along the direction of the magnetic field in the plasma. The width of the striation $\lambda_\perp$ is determined by the ionospheric conditions and the power density of the heating radiation.

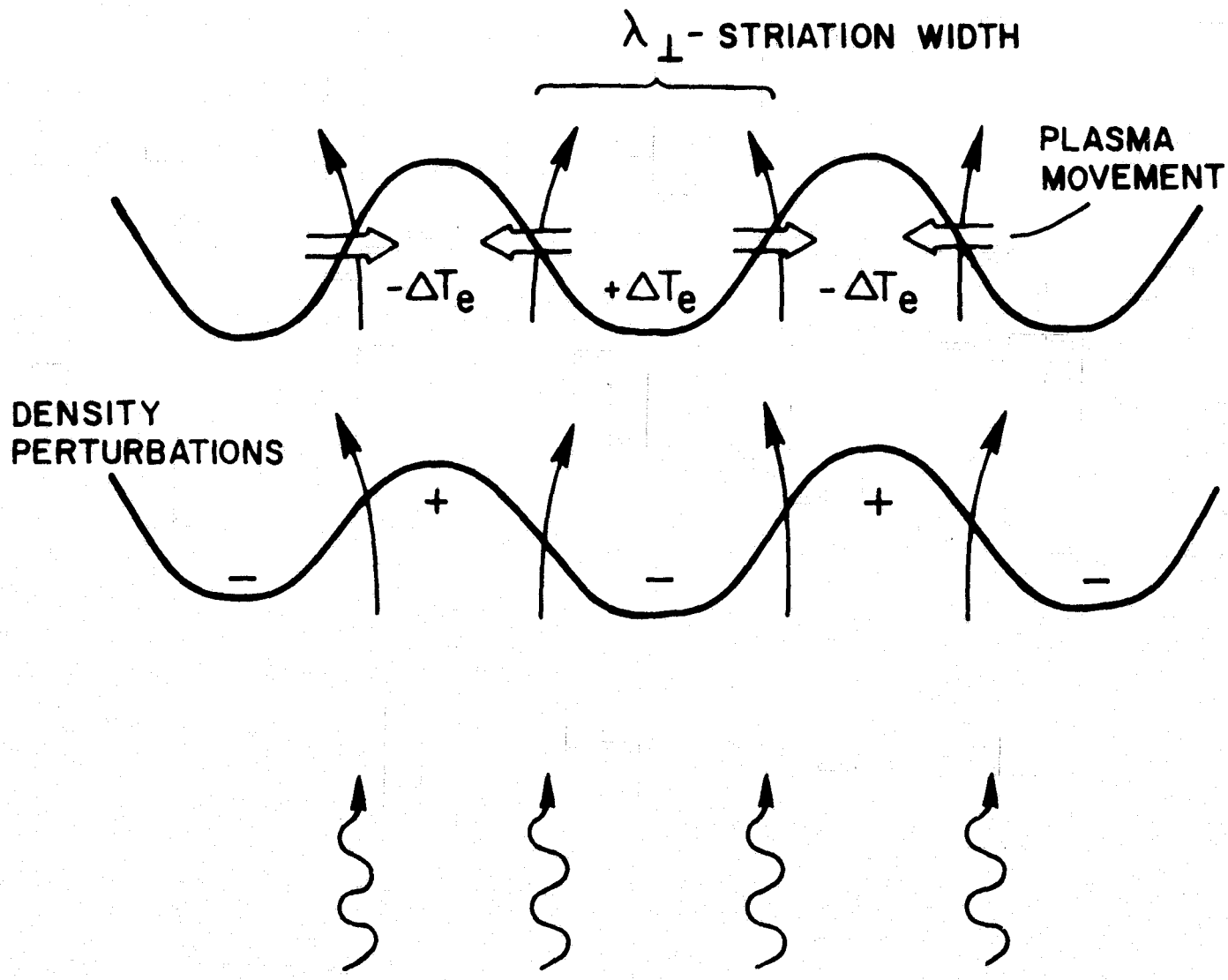
$\lambda_\perp$ - STRIATION WIDTH
PLASMA MOVEMENT
$-\Delta T_e$
$+\Delta T_e$
$-\Delta T_e$
DENSITY PERTURBATIONS
+
+
−
−
−
INCIDENT EM RADIATION

FIG. 3.1

It is not possible to determine a threshold power in the usual sense for thermal self-focusing because the threshold power depends on the striation width $\lambda_\perp$. According to the theory developed by Perkins and Valeo (1974), the threshold power density for underdense heating can be written as

$$P_{th} \simeq (1.2 \times 10^{23}) T_e^{\,5} f_o^{\,2} f_e^{-6} \lambda_\perp^{-4} \sin^2\varphi$$

where T_e is the electron temperature (°K), f_o is the frequency of the heating wave, f_e is the critical ionospheric frequency and φ is the angle between the electromagnetic wave vector and the magnetic field. This relationship is graphed in Figure 3.2 for two different operating frequencies, 2.45 GHz and 5.8 GHz, both with power densities of 20 mW/cm^2 in a typical daytime ionosphere.

This graph tells us what size striations will form for a given angle between the SPS beam and the magnetic field. It says nothing about the magnitude of the density fluctuations which make up these striations. In order to discuss the magnitude of the density fluctuations we must consider the spatial amplification of these fluctuations. Threshold conditions are obtained at the point where the density fluctuations are just maintained in space. If the spatial amplification is small then there will be no observable effect because the density fluctuations caused by the self-focusing instability, Δn_{sf}, will be much less than the natural fluctuation of the plasma, Δn_{nat}. In order to obtain a more meaningful threshold condition, we arbitrarily require that at least $\Delta n_{sf} \geq \Delta n_{nat}$.

If we require that $\Delta n_{sf} = 2(\Delta n_{nat})$ and that this amplification occurs within 5 scale heights of the ionosphere ($\sim$ 500 km), then the geometry restrictions are rather severe, as Table 3.1 illustrates.

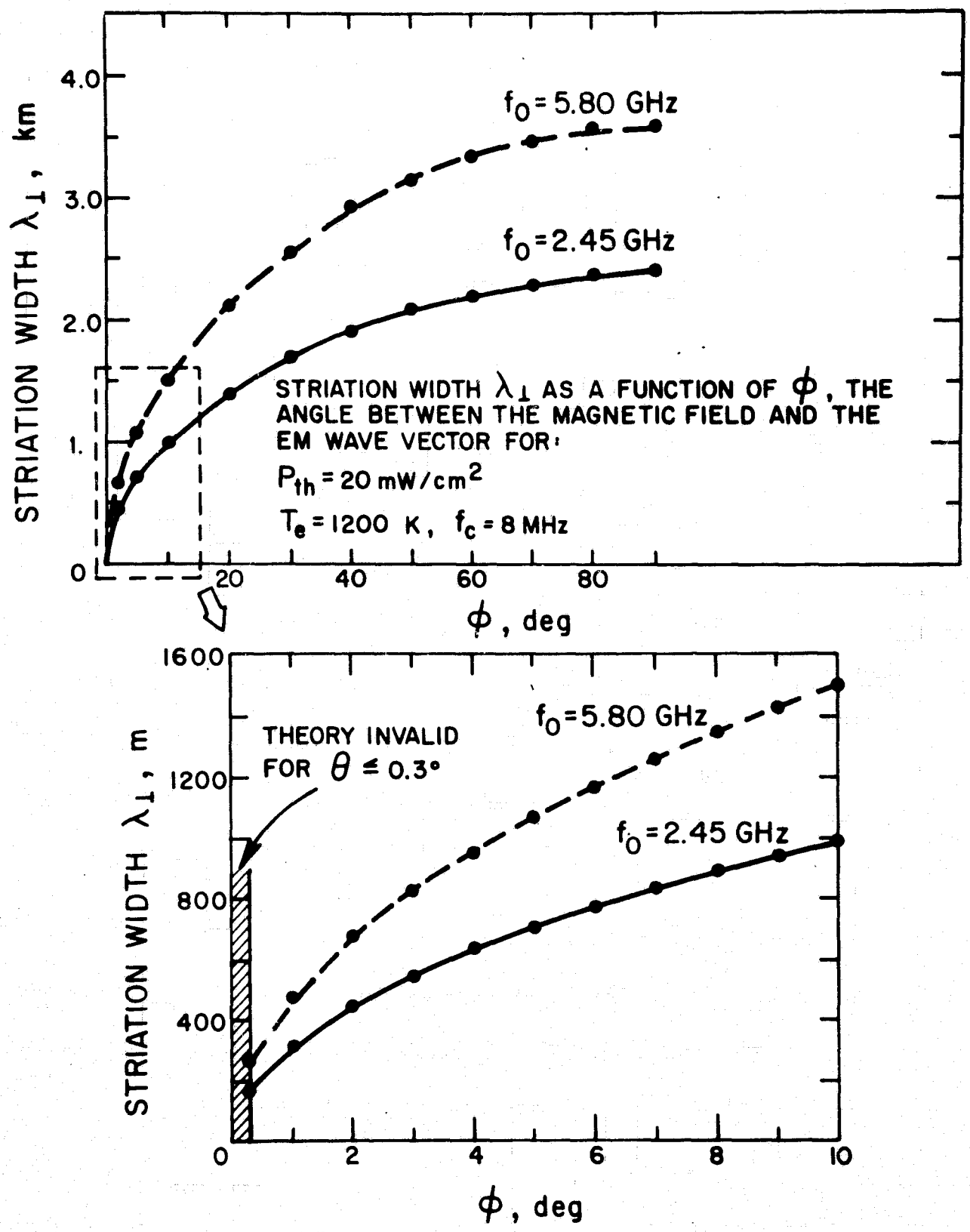

FIG. 3.2 THRESHOLD CONDITIONS

TABLE 3.1

Limiting angles, φ, for the formation of striations with width, $\lambda_\perp < 5$ km and $\Delta n_{sf} = 2(\Delta n_{nat})$

f_o (MHz)	Geometry Restrictions
2.45	$\varphi \leq 7.0°$
3.0	$\varphi \leq 4.6°$
4.0	$\varphi \leq 2.6°$
5.0	$\varphi \leq 1.6°$
5.8	$\varphi \leq 1.2°$

The equation which relates the limiting angle φ to the frequency for $\lambda_\perp < 5$ km and $\Delta n_{sf} = 2(\Delta n_{nat})$ is

$$\sin\varphi \simeq .73\, f_o^{-2}$$

where f_o is the heating frequency in MHz.

Because the horizontal dimensions of the SPS beam will only extend ~ 5 km in the ionosphere, the neglect of striations > 5 km is sensible. To have a significant impact, several striations should be formed inside the heated region. Therefore, it is probably more reasonable to consider only those striations $\leq$ 1 km. However, the values of Table 3.1 are approximately the same for the choice of $\lambda_\perp \leq 1$ km.

Figure 3.1, the graph of threshold conditions, shows that striations of $\lambda_\perp \leq 1$ km are possible only for $\varphi \leq 10°$ for $f_o = 2.45$ GHz or $\varphi \leq 4.5°$ for $f_o = 5.8$ GHz. These geometry restrictions would be even more severe if we consider the spatial amplification, as suggested by Table 3.1.

There is also growth in time given by $\Delta n_{sf} = \Delta n_{nat} e^{\gamma t}$, where γ is the growth rate. Because of the fading and rapid movements of the natural density fluctuations in the ionosphere, it is believed that only relatively large positive growth rates (corresponding to large striation widths) need be considered near threshold conditions. A more detailed analysis probably would place the geometry restrictions near those predicted in Table 3.1. The frequency scaling would be exactly the same, however.

These geometry restrictions imply that if the SPS microwave beam makes an angle less than φ to the magnetic field in the ionosphere then there is a possibility of striations occurring. This angle φ is related to the placement of the rectenna on the surface of the earth. Contours of constant φ can be drawn on the surface of the earth as shown in Figure 3.3 (Helliwell, 1977) and Figure 3.4. Placement of the rectenna outside the contours of the limiting φ for self-focusing would inhibit the striations from forming.

Observations of overdense thermal self-focusing have been reported for HF ionospheric modification experiments. The study of field-aligned irregularities in the overdense modified ionosphere was first undertaken by Thome and Perkins (1974) using a circular HF phased array at Platteville. His results confirmed that these striations formed with power densities and growth rates close to those predicted by Perkins and Valeo (1974). Results from a recent ionospheric modification experiment at Arecibo (Duncan and Behnke, 1978) have provided the first detailed observations of individual self-focused striations, as well as striation maps of the entire wave-plasma interaction region. These results, while in comparative agreement with theoretical predictions, suggest that additional plasma effects should also be considered.

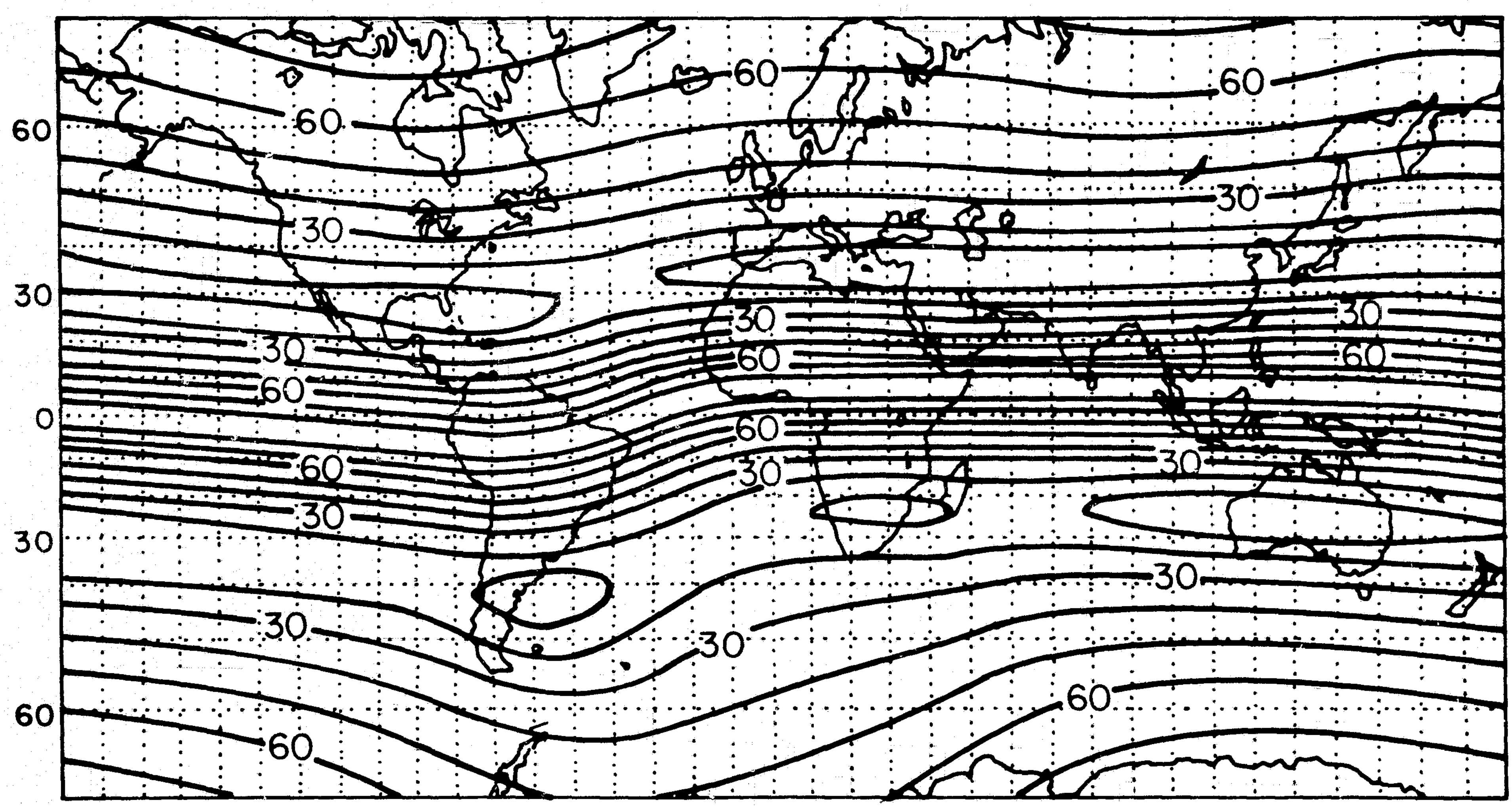

FIG. 3.3 SPS BEAM ANGLE TO MAGNETIC FIELD IN IONOSPHERE IN MAGNETIC MERIDIAN

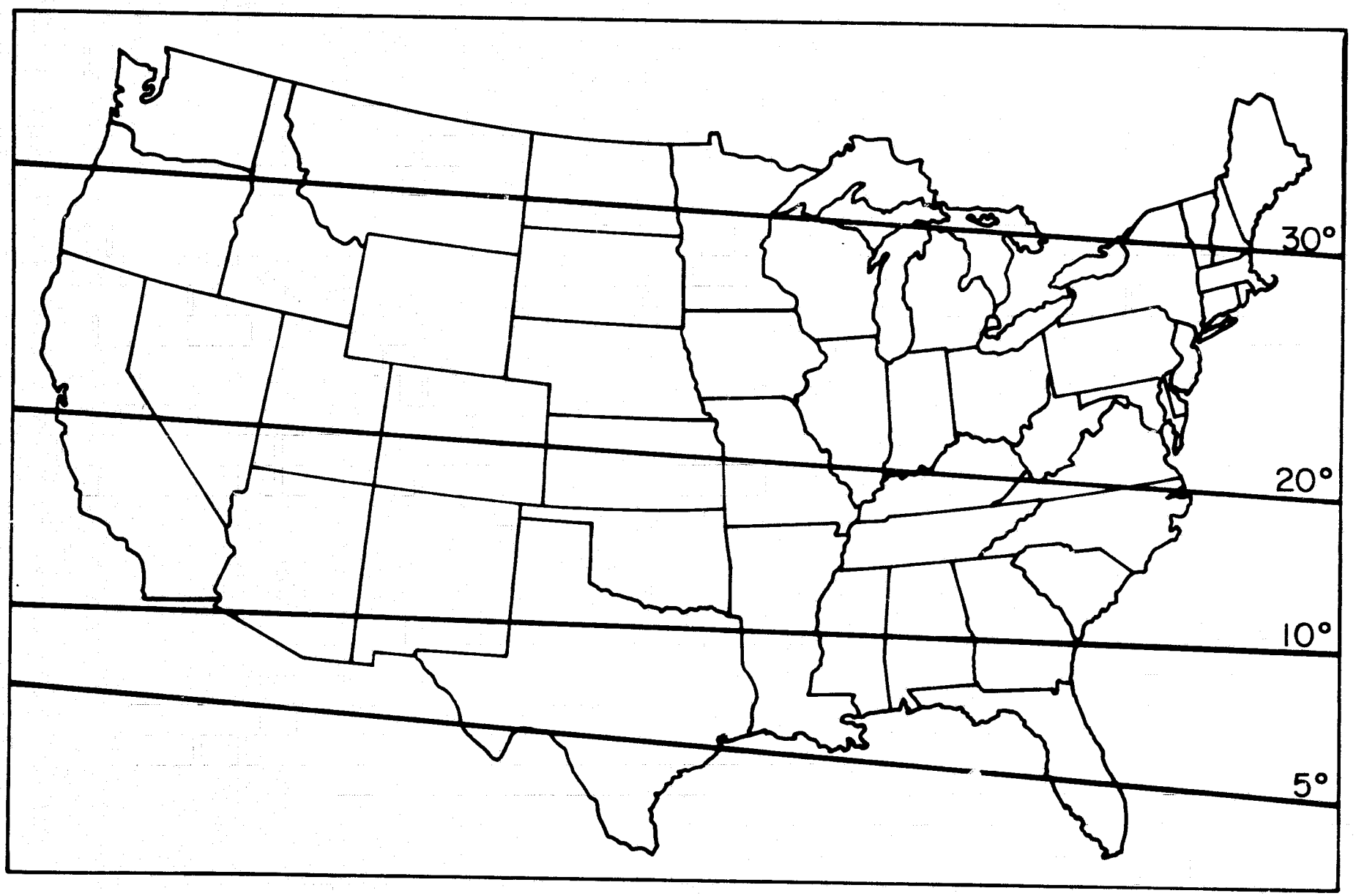

FIG. 3.4 APPROXIMATE SPS BEAM ANGLE TO THE MAGNETIC FIELD IN THE IONOSPHERE.

Intense high-frequency (HF) electromagnetic radiation incident on an overdense ionospheric plasma is known to excite parametric instabilities, enhancing electron plasma oscillations observable by incoherent backscatter radar (Carlson et al., 1972; Wong and Taylor, 1971). These instabilities continue to be the subject of intense experimental study. Of importance here is the fact that above instability threshold the strength of the enhanced plasma waves directly depends on the local power of the pump electric field. In addition, because of exact frequency and wave number matching conditions for both the parametric wave-plasma interaction and the radar incoherent backscatter process, these enhanced waves are detected at only one altitude. As a result, systematic scanning of the narrow radar beam across the interaction region of the enhanced plasma waves yields a two-dimensional cross-section characteristic of the local electric field intensity. These maps of electric field strength clearly show self-focusing striations and large-scale structuring of the illuminated plasma. Because the direction and rate of the radar scan are experimentally controlled, the cross-sectional dimensions of the individual striations are easily measured. Alternatively, if the radar is fixed, the irregularities follow a slow natural (E x B) drift through the beam, allowing a detailed study of the small-scale structure within individual striations. Once the irregularity size is determined, striation velocities can be calculated from these drift measurements. The experimental configuration is shown in Figure 3.5.

The data presented here were obtained during an ionospheric modification experiment conducted from 2 June to 17 June 1977 at the Arecibo Observatory (NAIC). The incoherent backscatter radar operates at 430 MHz with a 1/6° beamwidth, corresponding to approximately 730 meters at a

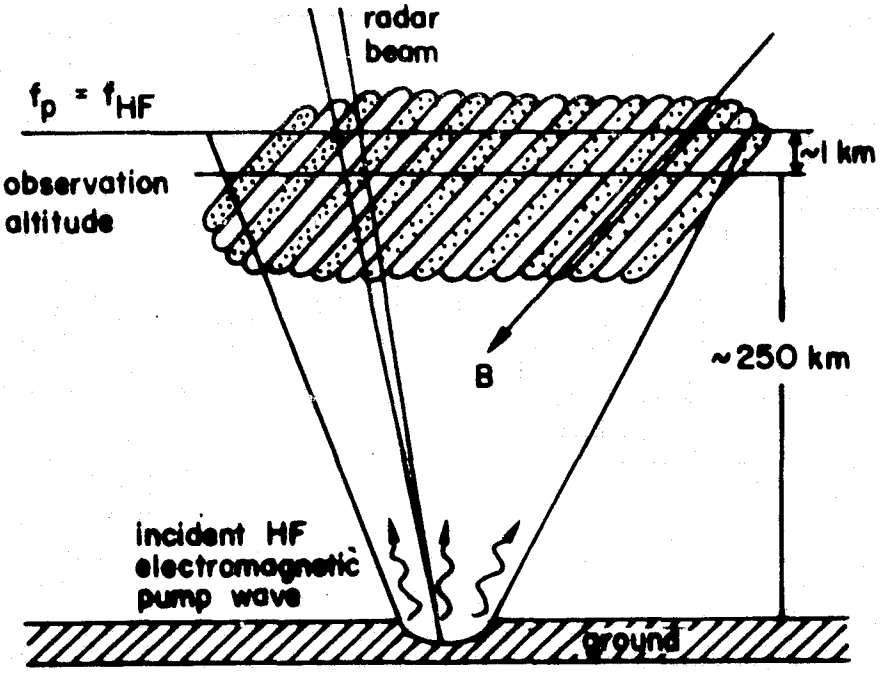

FIGURE 3.5 The experimental configuration for incoherent backscatter radar mapping of overdense self-focusing striations.

typical interaction height of 250 km. The HF wave beamwidth is a function of the operating frequency, ranging from 7.2° at 7.8 MHz to 10.9° at 5.185 MHz, or 31.5 km and 47.5 km, respectively, at 250 km altitude. The HF radiation is transmitted continuously with ordinary polarization and is fixed at vertical incidence, while the 430 MHz radar is pulsed and can be swept in zenith angle at a maximum rate of 1.87°/minute, or 136 m/sec at 250 km. The enhanced plasma wave intensities are measured over a 20 KHz bandwidth offset from 430 MHz by the HF pump frequency. A 500 μsec radar pulse is used with a pulse repetition period of 8500 μsec, as determined by the 6% transmitter duty cycle. The data rate is not continuous; data are accumulated in arrays of 1024 pulses after which there appears a data gap of approximately 0.4 sec in which the array is displayed real-time and recorded on magnetic tape.

Results of the two basic observing strategies are shown in Figure 3.6. The data in Figure 3.6a represent the natural drift of striations through the fixed radar beam. This drift gives rise to a slow regular modulation of the measured plasma line intensities, with typical periods of 60 to 90 seconds. Similar fluctuations have been noted previously without interpretation. The second data set, Figure 3.6b, was taken immediately following the above drift measurements and shows a series of distinct striations observed by rapidly sweeping the radar beam north across the interaction region. Typical striation dimensions deduced from observations over many such scans are 1.2 km in the north-south plane and 1.0 km in the east-west plane. Striation velocities are on the order of 25 m/sec, with components of 20 m/sec to the east, and smaller than 15 m/sec in the north-south direction. North-south velocity measurements are complicated by the strong

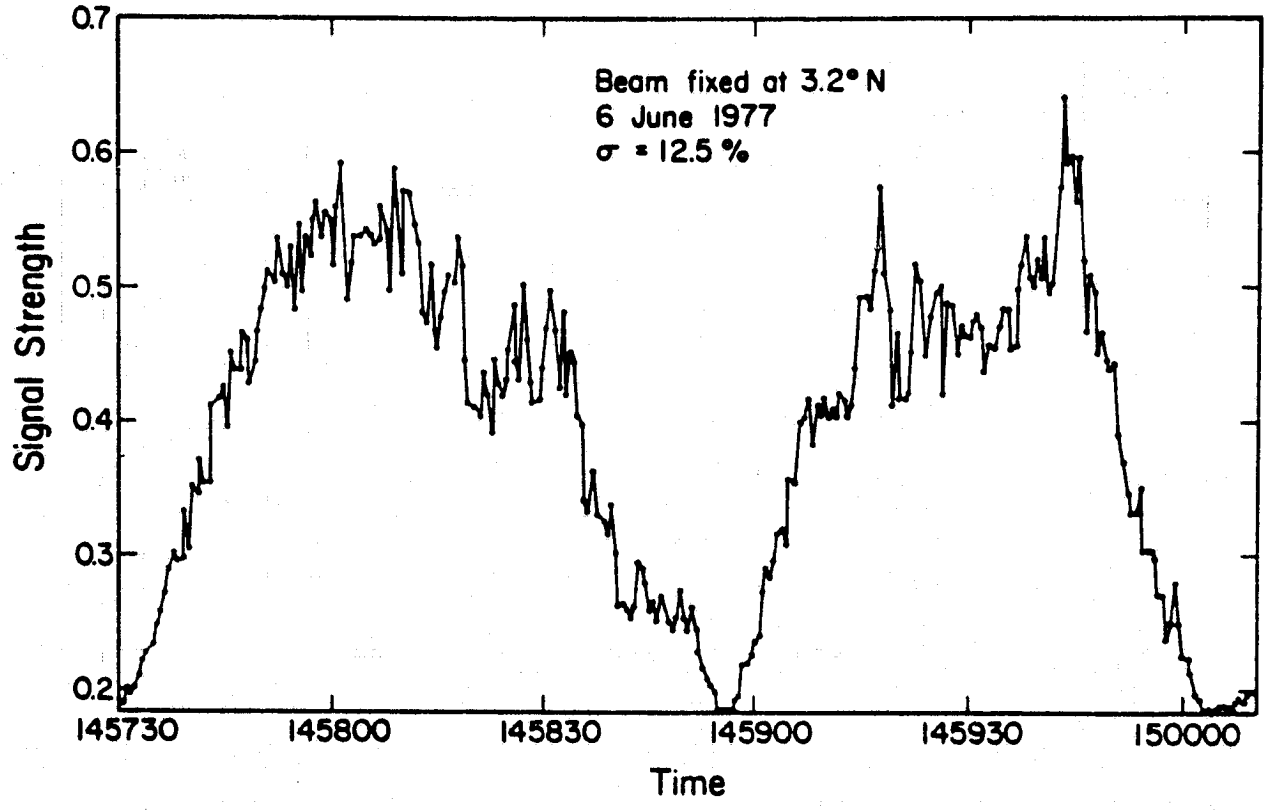

FIGURE 3.6a

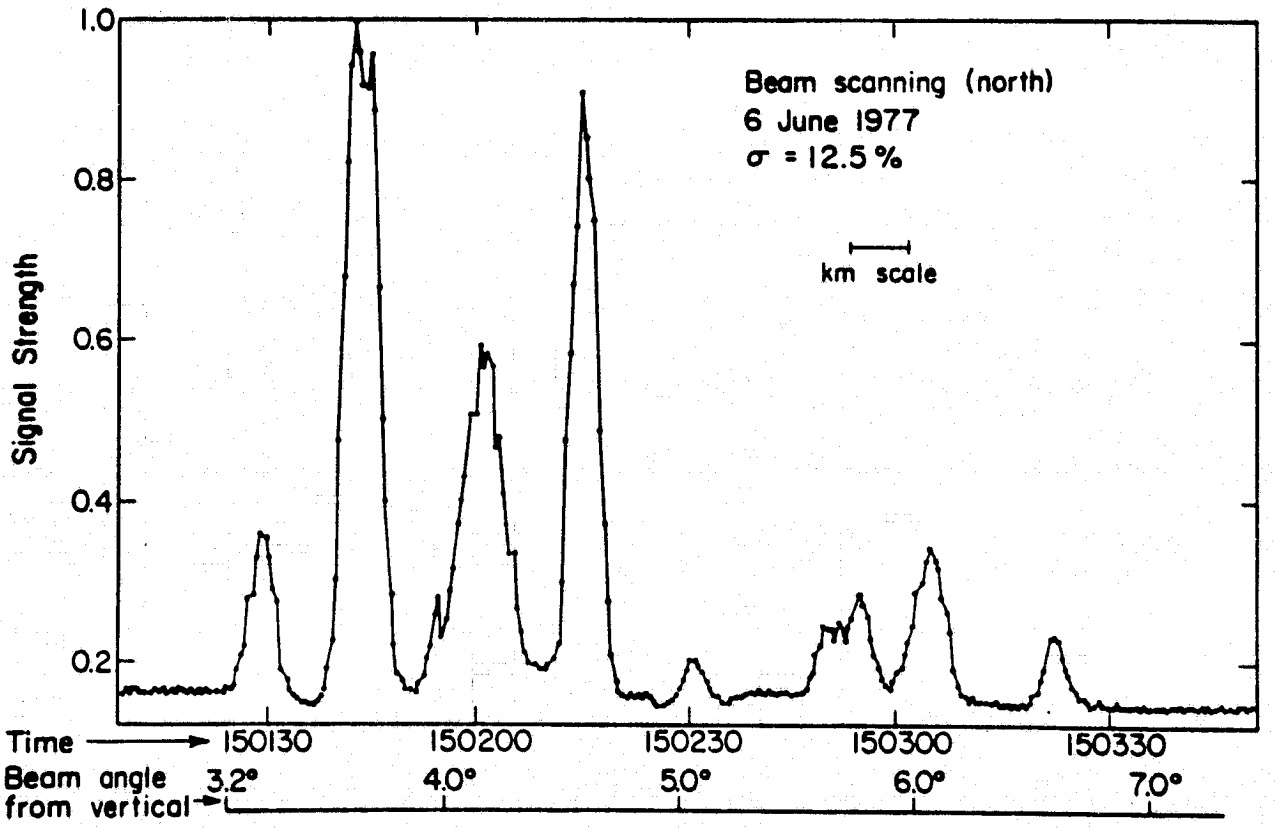

FIGURE 3.6b

spatial dependence of the striation width in the magnetic meridian plane.

A useful observing procedure is to scan the radar through a set of striations, quickly reverse the beam direction, and sweep back through the same striations. This yields a simultaneous determination of striation size and velocity in the scan direction. An example of data taken using this technique is shown in Figure 3.7. The striation widths and relative spacings are significantly effected by scanning with or against the component of the striations' drift motion. The data shown here clearly suggest a dominant drift movement to the east. The striation dimensions then can be calculated including a correction for velocity-induced measurement errors as well as allowing for the radar beamwidth. The lower limit for striation sizes thus measured is approximately 500 m.

The experimental observations are best explained by thermal self-focusing theory (Perkins and Valeo, 1974). For the conditions appropriate to an overdense ionospheric modification experiment, the instability threshold power density can be expressed as

$$P_{th}(W/m^2) \simeq (1.9 \times 10^{12})\, T_e^{5} \sin^2\varphi / L f_{HF}^{3} \lambda_\perp^{2} \quad ,$$

where T_e is the electron temperature (°K), L is the plasma scale height, f_{HF} is the pump frequency, $\lambda_\perp$ is the striation width, and φ is the angle between the electromagnetic wave vector and magnetic field. For typical experimental parameters, T_e = 1200°K, L = 100 km, f_{HF} = 8 MHz, and φ = 40° (vertical incidence at Arecibo), then

$$P_{th}(W/m^2) \simeq 38\, \lambda_\perp^{-2} \quad .$$

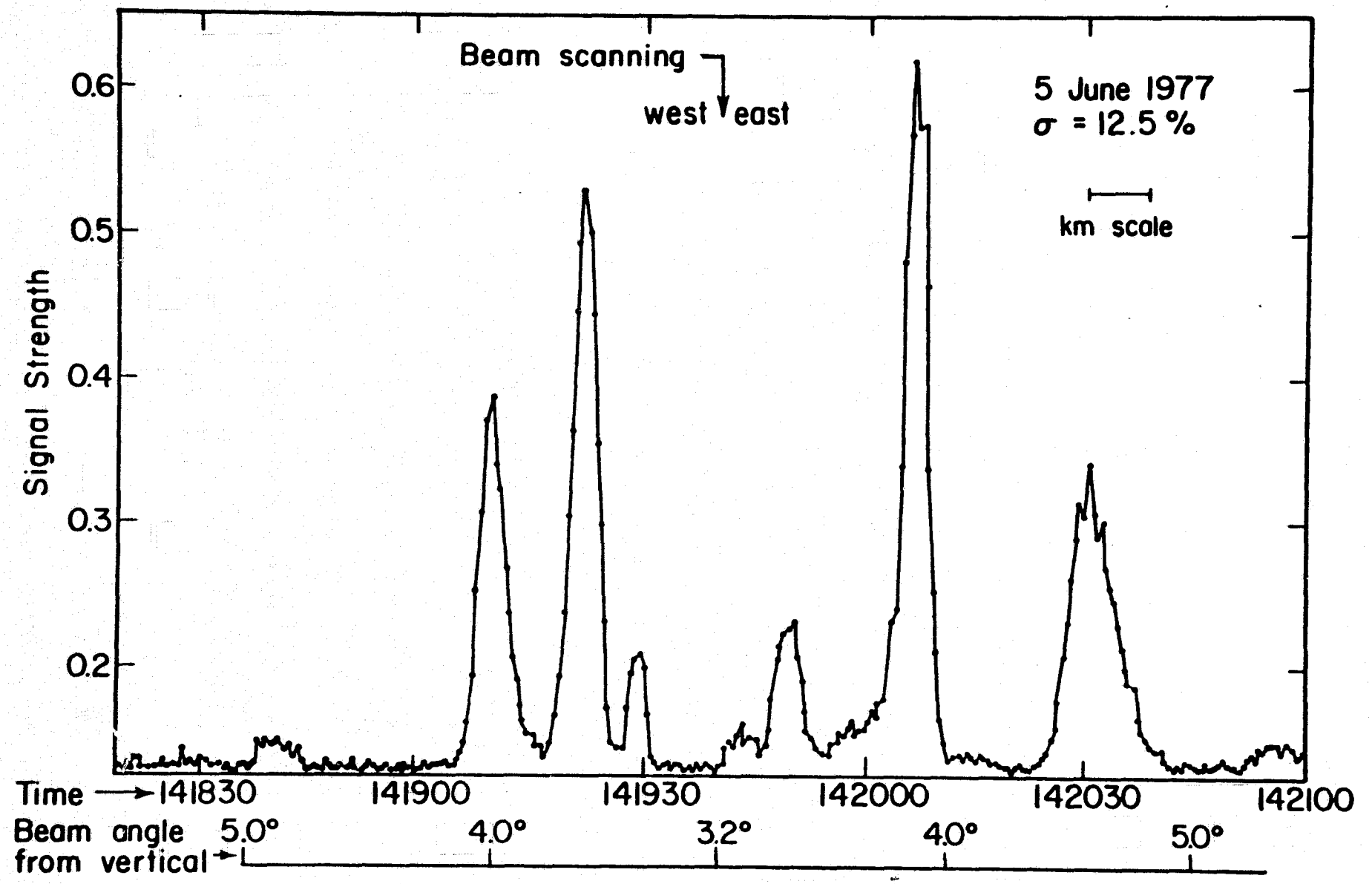
Beam scanning
west
east
5 June 1977
σ = 12.5 %
km scale
Signal Strength
0.6
0.5
0.4
0.3
0.2
Time → 141830
141900
141930
142000
142030
142100
Beam angle from vertical → 5.0°
4.0°
3.2°
4.0°
5.0°

FIGURE 3.7

The HF power density at 250 km can be estimated at 30 $\mu W/m^2$, yielding a striation width of $\lambda_\perp$ = 1.1 km. This agrees well with the experimentally measured values.

A more detailed comparison of experimental and theoretical striation dimensions is given in Figure 3.8. The pump power density is taken to be a gaussian distribution across the HF beam, causing the theoretically predicted striation width to increase with angle from vertical incidence. Additionally, in the magnetic meridian (north-south) plane, the angle between the HF wave vector and the magnetic field also is a function of beam angle from vertical incidence. These effects are combined to produce the theoretical curves shown in Figure 3.8, which again approximate the experimental data very well.

Although results of overdense self-focusing experiments agree with theory, underdense heating is sufficiently different that experimental work is needed to verify frequency and power density scaling relationships. No underdense self-focusing experiment has been attempted, primarily because diagnostics were not capable of detecting the large-scale irregularities should they form. A new technique is now being developed for future implementation at Arecibo.

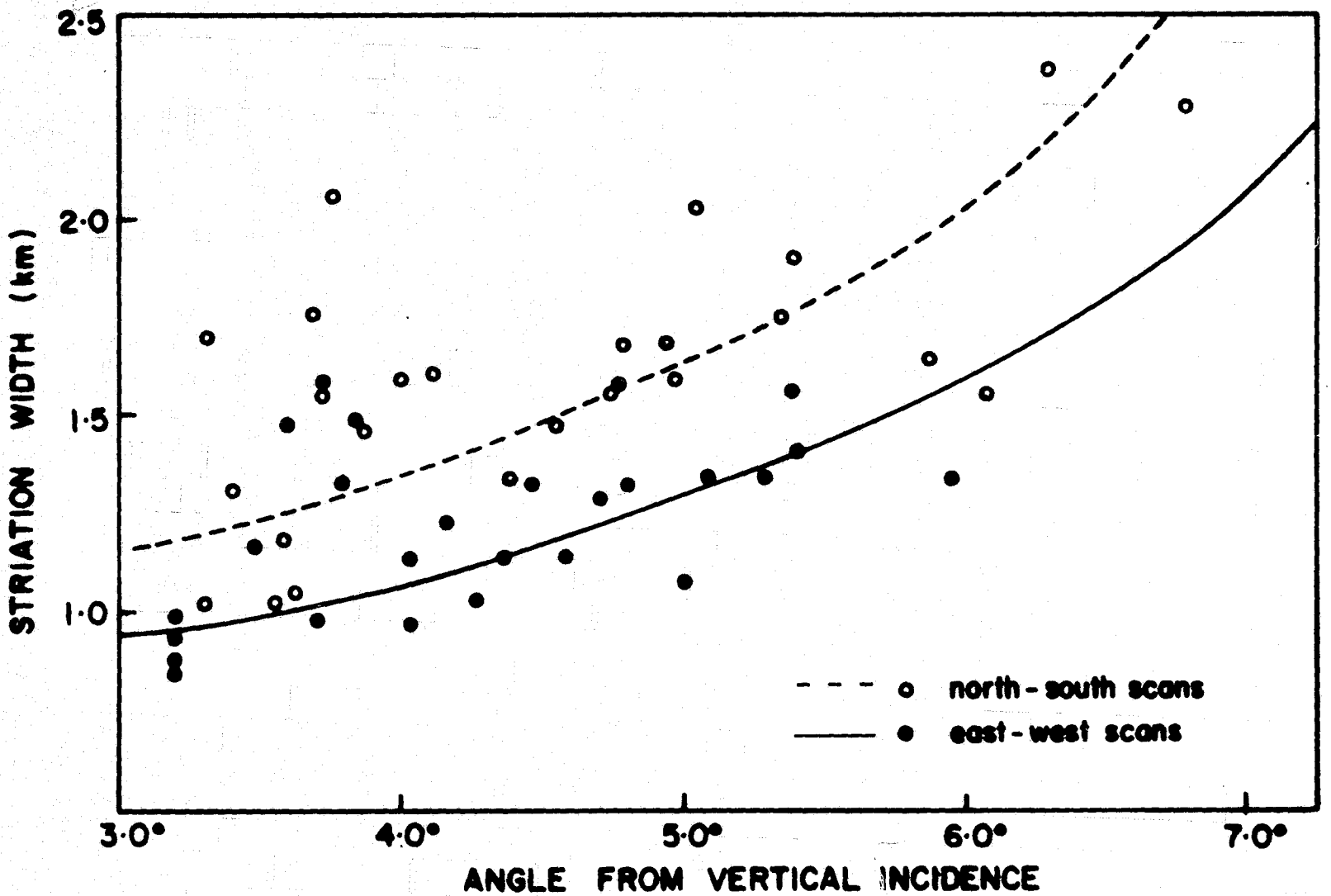

FIGURE 3.8 Variation of striation width as a function of power and θ - experiment and theory.

CHAPTER 4

FREQUENCIES 2450 MHz and 5800 MHz

Task: Document an analysis which continues the studies determining the power density levels at which nonlinear microwave/ionospheric interactions begin to occur. This analysis should include the IMS frequency bands around 2450 MHz and 5800 MHz.

4.1 Ionospheric Effects

Ohmic heating of the ionosphere is discussed in Section 3.1. For the purpose of comparing the frequencies 2450 MHz and 5800 MHz, the relevant result is that the energy deposited is inversely proportional to the operating frequency squared (Equation 1, Section 3.1). This result suggests that increasing the operating frequency has an important advantage in the ionosphere, in particular, changing from 2450 MHz to 5800 MHz reduces the energy deposited by the ohmic heating by the ratio of those frequencies squared or a factor of 5.6 for the same incident power density. This advantage may be applied in various ways. First, one could increase the power density by 5.6 at the higher frequency and produce the same ohmic heating effects, i.e., a five gigawatt system at 2450 MHz and a 28 gigawatt system at 5800 MHz produce the same effect on the ionosphere. If the five gigawatt system produces undesirable effects, the 28 gigawatt system will produce the same effects, no more no less. Second, if a five gigawatt system at 2450 MHz produced undesirable effects, a five gigawatt system at 5800 MHz might not produce undesirable effects since the heating is reduced by a factor of 5.6. Or better, if the threshold of the undesirable effects is determined experimentally then a system can be designed that would not

excite those effects, and the higher frequency system could operate at a higher power level for the same ionospheric heating.

Up to this point, we have considered the problem from the point of view of the ionosphere alone. The beam, of course, propagates not only through the ionosphere but also through the neutral atmosphere, including the troposphere, and one must ask what effects may be encountered in the neutral atmosphere.

4.2 Tropospheric Effects

The tropospheric propagation of microwaves has been under study since World War II and a great deal is known about the subject largely because of its importance in line-of-sight relay systems and for paths beyond the horizon (tropo-scatter systems).

For the purposes of the SPS study, one finds that the troposphere, like the ionosphere, is essentially transparent for microwaves but one should quickly note that there are tropospheric effects that occur when the frequency is increased. The effects are of two kinds: attenuation by the gases in the medium and attenuation by hydrometeors: rain, snow and hail. Attenuation of microwaves by water vapor and oxygen (Van Vleck, 1947a and 1947b) becomes important as the frequency increases beyond 10,000 MHz due to the electric dipole moment of the water vapor molecule and the magnetic dipole moment of oxygen. For frequencies below 10,000 MHz the attenuation from these gases is less than 10^{-2} db/km at sea level. The attenuations at 2450 MHz and 5800 MHz are nearly the same and about 7×10^{-3} db/km at sea level. Taking the equivalent thickness of the atmosphere to be 10 km, one finds that the attenuation through

the neutral atmosphere for a wave arriving from a geosynchronous satellite on the station's meridian at an elevation angle of 90° (at the equator) is 0.07 db at an elevation angle of 60° (at latitude ~ 33°) the attenuation is 0.08 db, and at an elevation angle of 30° (at latitude ~ 66°) the attenuation is 0.14 db. At the three elevation angles the neutral atmosphere losses for a five gigawatt beam are about 80, 90 and 160 megawatts, respectively. The losses quoted apply to the lower frequency; at the higher frequency the losses are higher by about 10 percent.

Attenuation by hydrometeors (Battan, 1973) occurs both by absorption and scattering of the incident energy. Measured attenuations by hydrometeors are available at wavelengths of 10 and 5.5 cm and these are representative of the frequencies 2450 and 5800 MHz. The values are 3×10^{-3} and 8×10^{-4} db/km per mm/hr of rainfall at wavelengths of 5.5 cm and 10 cm, respectively. A very heavy shower (rainfall of 25 mm/hr) from a storm through which the microwave beam has a long path (20 km) produces attenuations of 0.4 db at λ = 10 cm and 1.5 db at λ = 5.5 cm. Snow has a smaller attenuation rate than rain for a given precipitation measured in mm/hr but hail, particularly wet hail, can produce more serious effects when it falls through the microwave beam, and the effects are illustrated in Table 4.1 (taken from Battan, 1973, Table 6.5, p. 81).

TABLE 4.1

Attenuation in db/km for Spherical Hail Coated with Liquid Water

Maximum Hail Diameter	Wavelength = 5.5 cm			Wavelength = 10 cm		
	Coating of Water			Coating of Water		
	dry	0.01	0.05 cm	dry	0.01	0.05 cm
0.97 cm	0.015	0.19	0.56	0.002	0.05	0.058
1.93 cm	0.18	0.79	2.48	0.017	0.15	0.34
2.89 cm	0.33	1.12	2.82	0.034	0.19	0.60

4.3 Attenuation by Hail

If a hail storm has a length of 10 km along the microwave beam then the attenuations per kilometer in the table are multiplied by 10. The advantage of the lower frequency (longer wavelength) is apparent. Note that for large (2.89 cm diameter hailstones) dry hail the attenuation is 3.3 db at λ = 5.5 cm and 0.34 db at λ = 10 cm. For large wet hail most of the energy is absorbed or scattered out of the beam and does not reach the rectenna. While the effect is more severe at the higher frequency (λ = 5.5 cm) the effect at the lower frequency (λ = 10 cm) is serious (less than 10% of the energy gets to the rectenna). It is therefore of interest to look at the frequency of occurrence, variability in time, and space of hailstorms.

4.4 Characteristics of Hailstorms

Most locales in the United States experience two or three hailstorms per year and of these only five to ten percent ever produce serious damage to crops, i.e., are intense hailstorms. The average number of days with hail at any point and the average intensity of hail is shown in Figure 4.1 (taken from Farhar et al., 1977, Fig. 1, p. 2). The frequency of occurrence at a point and the variability across the country are better illustrated by Figure 4.2 (taken from Changnon et al., 1977, Fig. 4, p. 10) which provides more detail than Figure 4.1.

Except for the isolated hailstorms near mountains, most hailstorms are associated with frontal activity on the weather map, particularly with rapidly moving cold fronts. These factors are reflected in the distribution shown in Figure 4.2.

The intensity of hail varies geographically (Changnon and Stout, 1967), being heavier in eastern Colorado (near the mountains) than in the midwest. As an illustration, note that Illinois hailstorms average 24 stones per square foot with only about two percent larger than a half-inch diameter, whereas in northeast Colorado the average is 202 stones per square foot with fifty percent larger than a half-inch.

Season is important. East of the great plains the maximum hail activity is in the spring, starting in March in the far south and moving to May in the northern states. In the mountain-lee the maximum activity is in the summer. Around the Great Lakes the maximum is in the fall. Some West Coast areas have maximum in late winter or spring.

Time of day matters. Few hailstorms occur between 5:00 and 10:00 AM local time. Near the mountains (Denver)

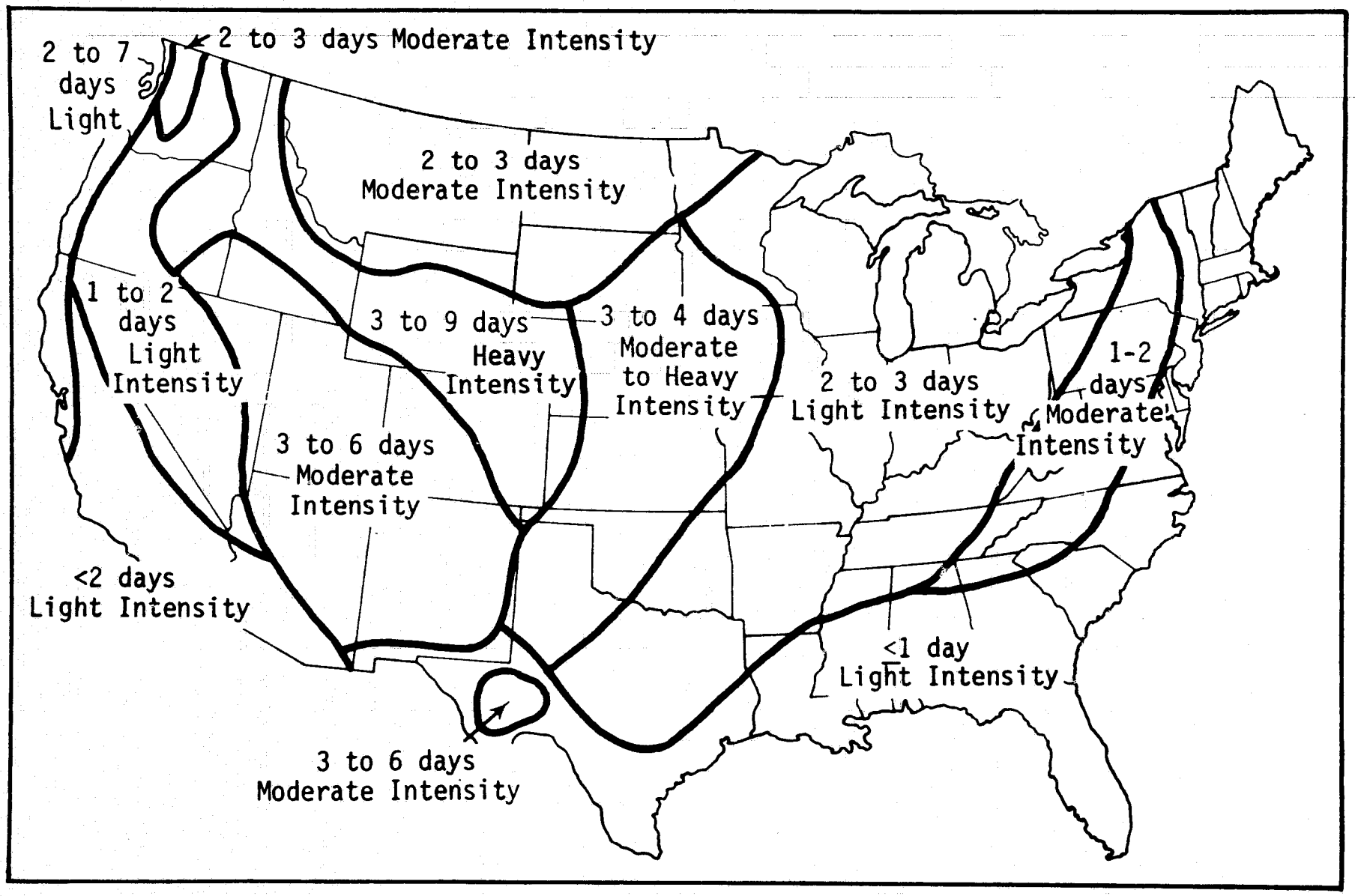

FIGURE 4.1 Average Annual Number of Days with Hail at a Point

FIGURE 4.2

Average annual number of days with hail at a point

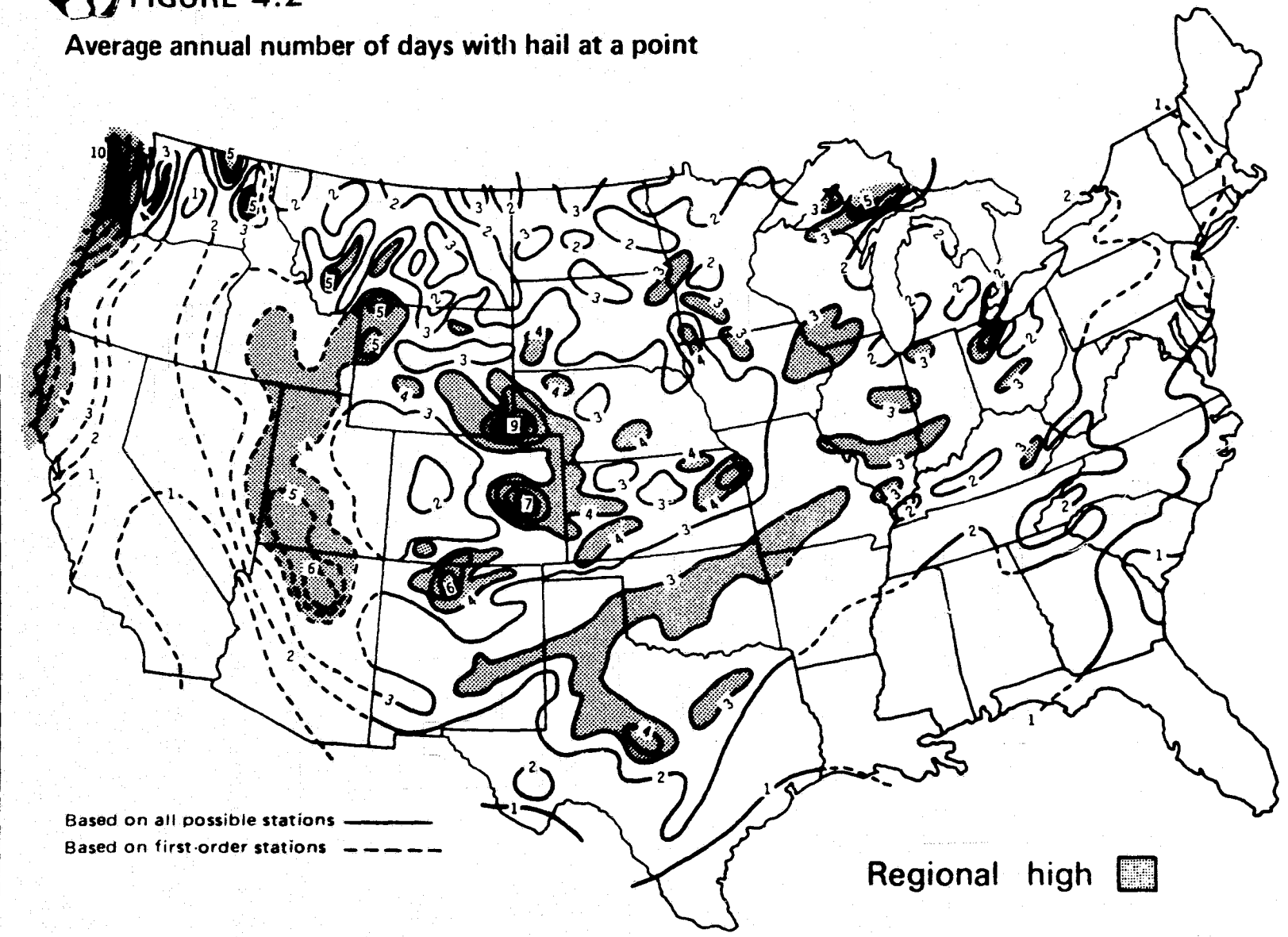

Note: The lines enclose points (stations) that have equal frequency of hail days

they often occur between Noon and 3:00 PM, a few hundred miles east of Denver between 3:00 and 6:00 PM, near Kansas City between 6:00 and 9:00 PM and in Illinois and the midwest generally between 2:00 and 5:00 PM and between midnight and 3:00 AM.

The duration of a hailstorm averages ten to fifteen minutes near the mountains, three to six minutes in the midwest.

The hail situation is summarized in Figure 4.3 (taken from Changnon et al., 1977, Fig. 7, p. 15) and by Changnon (1975) by dividing the country into thirteen regions and indicating for each region the basic cause of the storm, the number of storms per year, the peak season, and the intensity of the storms.

4.5 SPS Power Losses in the Atmosphere

To sum up, the losses are tabulated in Table 4.2 for the ionosphere, for the (neutral) atmosphere, and for rain and hail for the two frequencies. The losses in the table are the power lost from a five gigawatt SPS beam in traversing the medium. Any attempt to balance the losses is heavily dominated by the tropospheric effects and calls for the lower frequency.

FIGURE 4.3

Hail regions of the United States

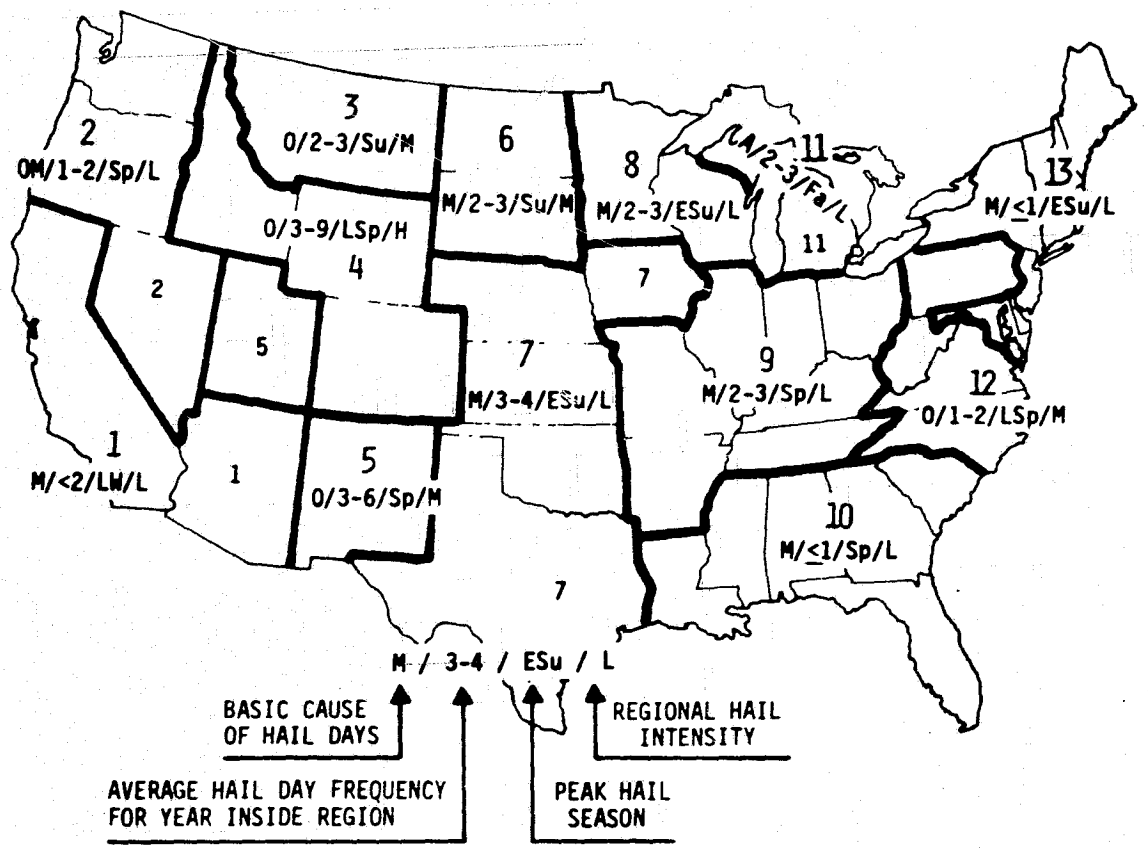

A=Marine, M=Macroscale, O=Orographic

E=Early, L=Late, Fa=Fall, Su=Summer, Sp=Spring, W=Winter

L=Light, M=Moderate, H=Heavy

TABLE 4-2

Estimates of 5 Gigawatt System Losses

Medium		2450 MHz	5800 MHz
Ionosphere		0.25 KW	1 KW
Neutral Atmosphere at 60° elevation angle		90 MW	100 MW
Rain (25mm/hr over 20 km path in beam)		45 MW	1.450 GW
Hail (1.93 cm diameter hailstones, 10 km path through the beam)	dry	0.2 GW	1.7 GW
	wet	2.7 GW	4.99 GW

It is clear that whereas the ionospheric effects argue for a higher frequency to reduce the ionospheric heating, the tropospheric effects argue for a lower frequency to reduce the power losses. These factors, (a) reducing the ionospheric heating with whatever effects it may produce and (b) reducing the losses by attenuation of the SPS beam in the atmosphere, are difficult to weigh. Until the ionospheric heating effects as a function of deposited energy or frequency are determined the choice cannot be made.

CHAPTER 5

PERTURBATIONS OF THE UPLINK BY A HEATED IONOSPHERE

Task: Document an analysis of the phase perturbations on the uplink pilot beam induced by the heated ionosphere. If these perturbations exceed 2 to 3° RMS, possible methods to minimize these errors shall be reported.

5.1 Introduction

The uplink pilot beam of the SPS is intended to provide a source of phase information used in forming the SPS microwave beam and directing the beam toward the proper rectenna. The pilot beam transmitter is located at the center of the rectenna and operates on a pair of sidebands equally spaced from the microwave beam frequency. The sidebands are sampled at a number of receiving elements distributed over the SPS transmitting antenna and combined to derive signals at the beam frequency. The phase of the received signal at a given point is compared with the phase at a reference point and the phase difference is used to adjust the phase of the local SPS transmitters. Thus, a phase distribution for the SPS transmitting antenna is produced and this distribution forms the SPS beam and aims it at the proper rectenna.

A comparison of the geometries of the uplink pilot beam and the downlink microwave beam is instructive. It is illustrated in Figure 5.1 but not shown to scale. For a rectenna in the southern United States the distance to the ionosphere from the rectenna is about 400 km and to the SPS about 40,000 km. The two rays from the pilot transmitter to the edges of the SPS antenna are only separated by 10 meters in the ionosphere, whereas the rays connecting the

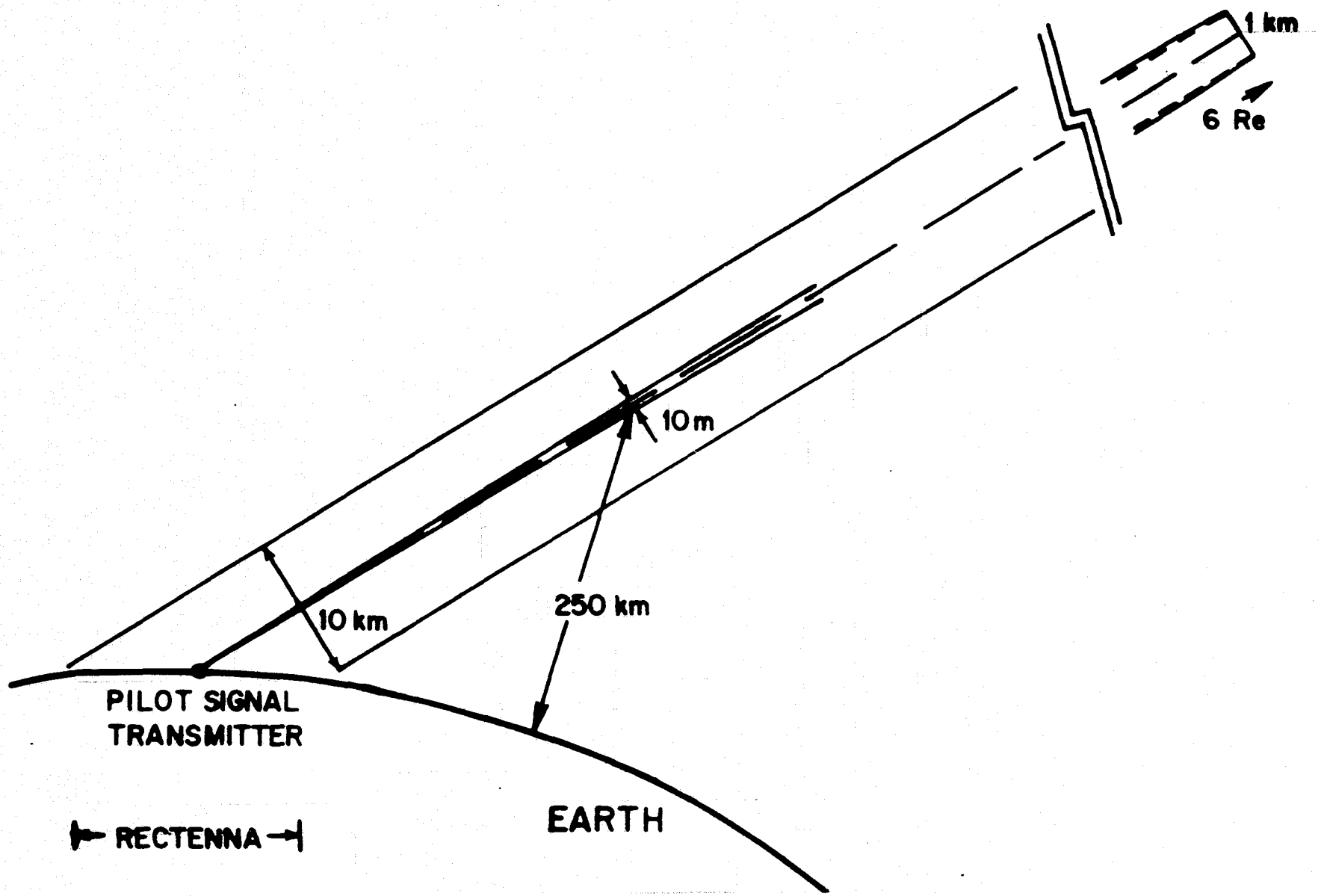

FIG. 5.1 DOWNCOMING SPS BEAM AND UPGOING PILOT SIGNAL BEAM

edges of the SPS antenna with the edges of the rectenna are separated by about 10 km in the ionosphere. On the basis of ray theory, then, the uplink pilot beam "sees" or propagates through only a small cross-section of the ionosphere that is traversed by the (downlink) SPS microwave beam. In no sense are these reciprocal propagation paths.

Ray theory will apply if the perturbations introduced by the medium are small. If the perturbations are large, then a full wave solution to the propagation problem (or a better approximation than ray theory) is in order. In this case the uplink transmission will be influenced by more than the 10 meter circle estimated for ray theory and the increased cross-section will depend on the precision of the theory required. (The first Fresnel zone has a diameter of 400 meters; the important scale in thin screen diffraction is 50 meters.) In any practical case the cross-section will be limited in size to less than 400 meters and more nearly 10 meters or a few tens of meters.

A physical picture of the perturbation of the uplink pilot beam is readily available. One can think of the shimmering of the image of an object seen through the turbulent eddies of a hot pavement. The object may be discerned but its shape is altered in a random way that varies with time. Through a heated ionosphere the SPS will see a pilot transmitter whose position dances with time. If the apparent departure of the transmitter from its true location is small, the effect is tolerable and it is possible to define small and tolerable in terms of energy lost from the system by the beam's spilling over the edge of the rectenna.

The problem, then, is to determine what is the effect on the uplink pilot beam of an ionosphere heated by the SPS microwave beam. Will the phase fluctuations observed at the receiving sites on the SPS be large enough to cause the beam

not to form, or to misalign the beam? This is the problem contemplated in the contract task and defined at a phase fluctuation of 2 or 3 degrees RMS. In pursuing the study we have uncovered a related problem. Simply stated, one must be certain that the uplink pilot frequencies are far enough removed from the downlink SPS frequency that the frequency differences do not pump the ionospheric plasma exciting parametric instabilities, for these are known to produce field-aligned striations that have significant effects on communications. This problem can be avoided if the frequency separation between the uplink and downlink exceeds twice the expected highest ionospheric plasma frequency. The ionospheric plasma frequencies are well known for a large number of stations and the data are catalogued in the World Data Centers. Fifteen or 20 MHz would probably be safe values to use as the expected highest plasma frequency, although the values should be checked against the data. Therefore, the sidebands on the uplink should be 30 to 40 MHz away from the downlink frequency for a sideband separation of 60 to 80 MHz and this requirement should be examined by the system people.

5.2 Observations of Ionospheric Perturbations of Microwaves

The surprising scintillation of communication satellite signals at gigahertz frequencies observed at ground stations has been reported and summarized by Taur (1976,1977). The early observations are found in COMSAT memoranda and in the COMSAT Technical Review.

Scintillations of radio signals propagating through the ionosphere are observed at all frequencies, but the scintillation amplitudes decrease rapidly (fading amplitude/signal amplitude proportional to inverse frequency squared)

and it was thought that by assigning satellite communication channels in the microwave region of the radio spectrum the problem would be avoided.

The installation of satellite communication systems at 4 and 6 GHz demonstrated that scintillations (peak-to-peak excursions up to 10 db) did occur at times in the tropics, the preferred times being early evenings in the months near the equinoxes. The occurrence of scintillations has been well mapped observationally in latitude, time of day, and season.

Aarons (1978) has provided the chart (Figure 5.2) giving the frequency of occurrence of scintillations greater than 2 db at Huancayo, Peru (geomagnetic latitude 0°) observed over a period of a year.

Microwave scintillations are observed in the tropics and in northern latitudes associated with aurora (Pope and Fritz, 1970). Taur (1974) suggests that the scintillations are within 25° latitude during periods of maximum solar activity and within 20° during periods of minimum solar activity. Scintillations are observed at a given station on more days during the preferred periods when solar activity is high. The aurora region is far enough north to be of no immediate interest for the SPS problem.

Figure 5.3 (taken from Taur, 1977, Fig. 2.1) shows a power spectrum of the fading of a 4 GHz signal measured at Hong Kong in September 1973, which Taur describes as typical. Note that the fading is largely in the frequency band 1/16 to 1/8 Hz (fading periods 8 to 16 seconds).

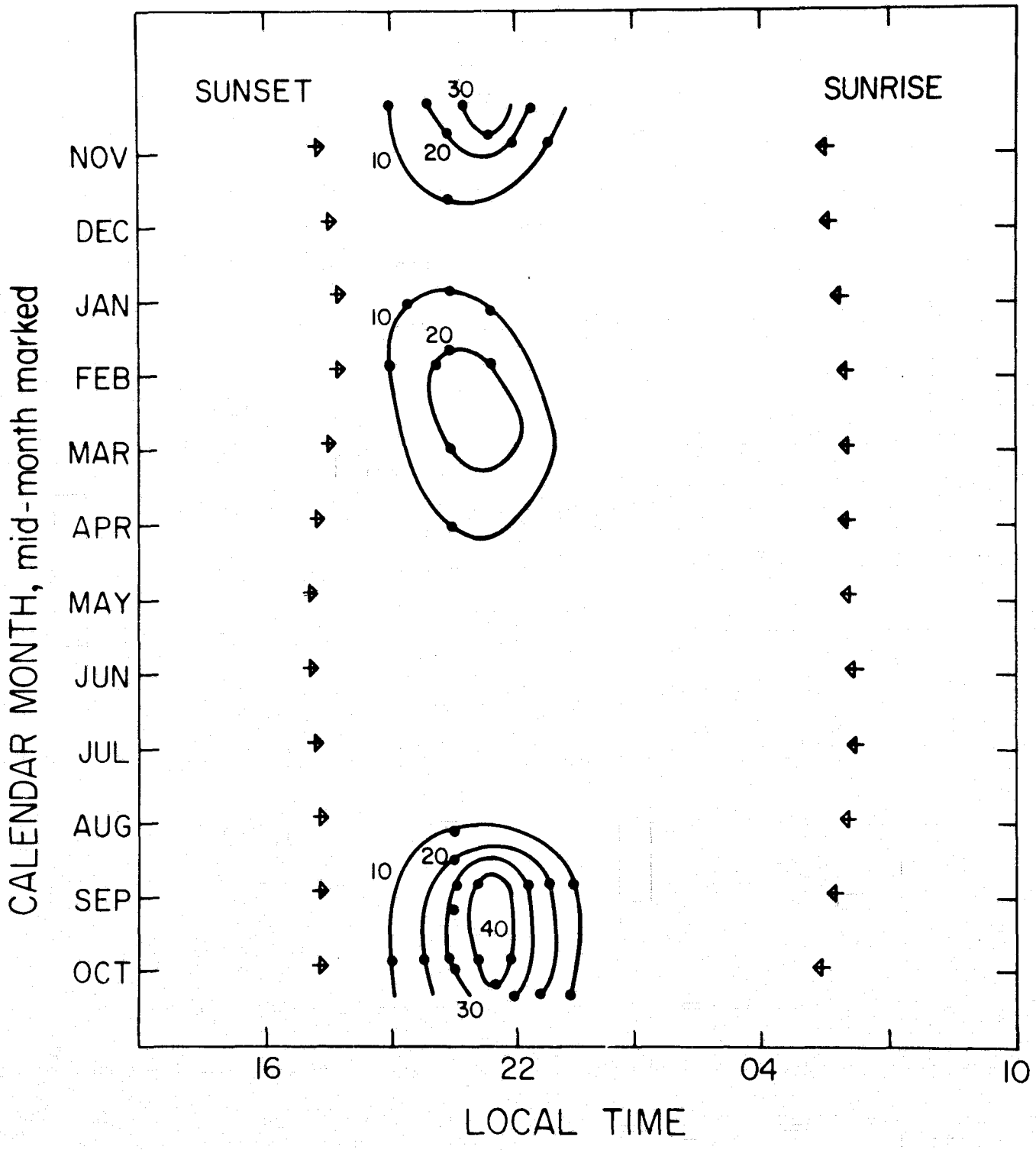

FIG. 5.2 DATA: HUANCAYO, PERU, APRIL '76 - MAR. '77, 1.4 GHz
CONTOURS ARE % OCCURRENCE OF SCINTILLATION $>$ 2 dB.

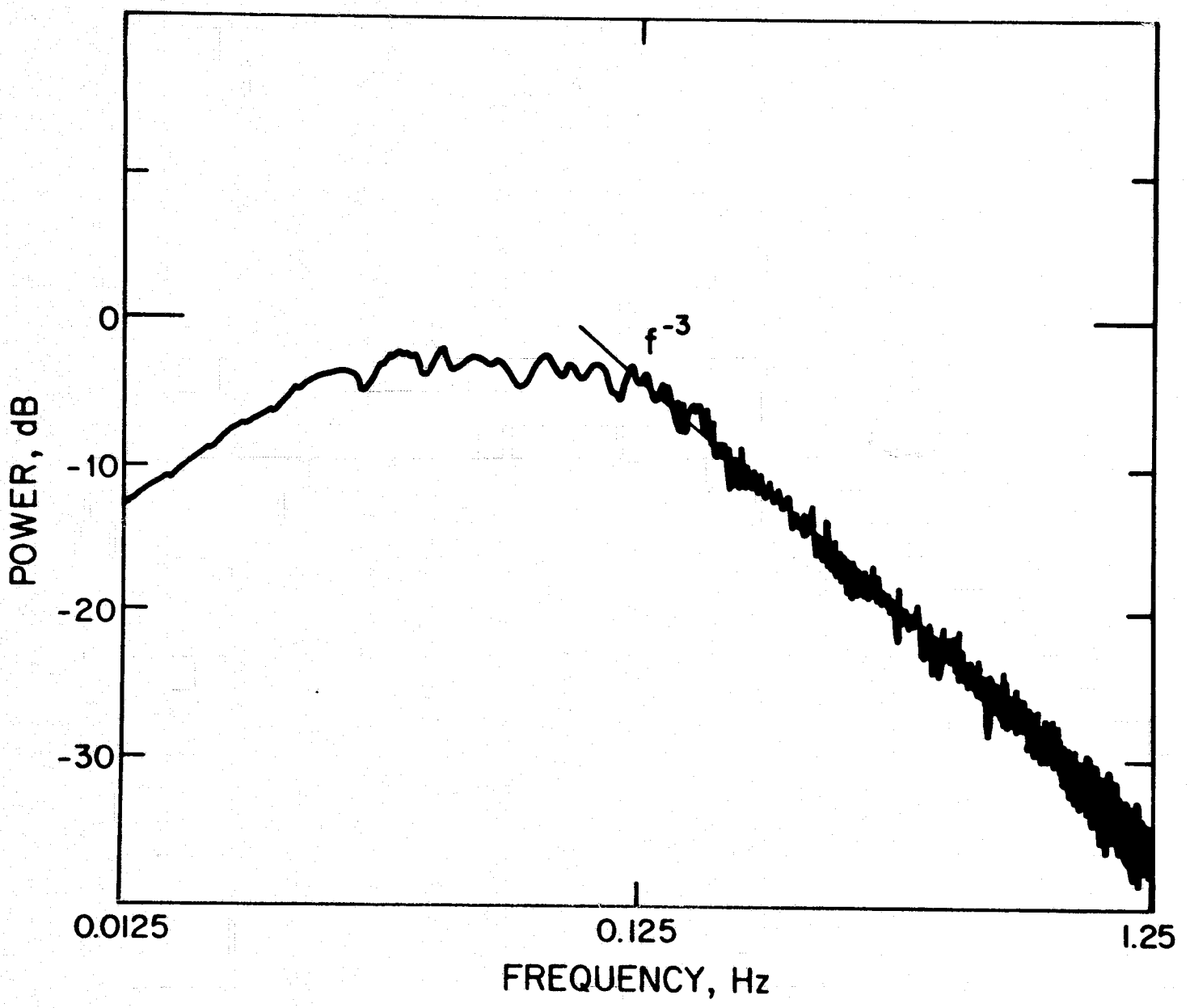

FIG. 5.3

5.3 Theory of Ionospheric Scintillations

Ionospheric scintillations are a feature of signals at 30-300 MHz and higher and various theories have been invoked to describe, among other things, the scintillation amplitudes as a function of frequency (scintillation amplitude is inversely proportional to frequency squared). The scintillation is the result of scattering by irregularities in ionization density in the ionosphere, with large scale irregularities behaving like lenses, and small scale irregularities as Rayleigh scatterers. The literature documents the work in detail, for example, see Booker (1975), Crane (1976), Rino (1976) or Rino and Fremouw (1977) for further references.

Several attempts have been made to explain the scintillation of microwave signals by the ionosphere (Wernik and Liu, 1974; Booker, 1975; Yeh, Liu and Youakim, 1975; Basu, Basu and Khan, 1976; Liu and Yeh, 1977; Booker and Miller, 1978). No generally accepted theory has yet emerged, and Booker and Miller (1978) conclude that there is no likely combination of ionospheric parameters that permits the explanation of gigahertz scintillation in terms of the theory of diffractive scattering caused by weak irregularities. A promising entry (Crain and Booker, 1978) will appear shortly. This explanation, called refractive scattering, has yet to be given a critical review. Refractive scattering is the reflection at grazing incidence of a radio ray by refractive index structure perpendicular to the line-of-sight. One can imagine a ray being reflected by a cylindrical irregularity as the ray grazes the surface of the cylinder. If the cylinder is not far off the direct line-of-sight, the angles of incidence and reflection are nearly 90 degrees requiring only small changes in refractive index (the angle of incidence exceeds the critical angle) and the important scale now is

the distance the refractive scatterer is off the direct path, rather than the size of the scatterer. There is a relation then between this scale and the change in refractive index needed to produce reflection. These ideas are developed by Crain and Booker (1978) who conclude that refractive scattering can explain strong scintillation of microwaves by the ionosphere. The Crain and Booker argument is outlined below.

Scintillation of radio waves propagating through an ionosphere containing irregularities arises from two phenomena: diffractive scattering and refractive scattering. Diffractive scattering is important if the scale T_D of the irregularity normal to the line-of-sight is a Fresnel zone, i.e.,

$$T_D = (\lambda d/2\sqrt{2}\ \pi)^{\frac{1}{2}}$$

where λ is the radio wavelength and d is the distance of the irregularity to the receiving terminal (for the SPS problem the transmitter can be assumed to be at a very large distance from the ionosphere so that a plane wave impinges on the ionosphere). If the ionospheric irregularities have scales equal to or less than T_D then diffractive scattering is important. If the scales are larger than T_D, diffractive scattering will be dominated by refractive scattering provided the scale associated with refractive scattering T_R is larger than T_D.

The refractive scattering scale T_D is the displacement normal to the line-of-sight of a scatterer for which the incident angle exceeds the critical angle of optics, θ_c, given by

$$\sin \theta_c = (n - \Delta n)/n$$

where n is the refractive index of the medium and n - Δn is the refractive index of the scatterer. The critical angle is quite insensitive to the form in which the refractive index changes from n to n - Δn. The grazing angle α is the complement of the critical angle, and the displacement of the scatterer from the line-of-sight at a distance d from the receiver is 2 αd.

$$\cos \alpha = 1 - (\Delta n/n)$$

$$\alpha^2 = 2(\Delta n/n) \text{ for small angles.}$$

For fluctuations in electron density N,

$$\alpha = \frac{\lambda}{\lambda_N} \left\{ \overline{\left(\frac{\Delta N}{N}\right)^2} \right\}^{1/4}$$

where λ_N is the wavelength associated with the plasma frequency.

The displacement from the line-of-sight of a scatterer that just satisfies the critical angle condition is T_R.

$$T_R = 2\alpha d = 2d \frac{\lambda}{\lambda_N} \left\{ \overline{\left(\frac{\Delta N}{N}\right)^2} \right\}^{1/4}$$

For irregularities having scales between T_D and T_R, assuming $T_R > T_D$, a modified ray theory is used by Crain and Booker to show that refractive scattering can produce the observed scintillations.

For the SPS case, T_D is about fifty meters and T_R is about 100 meters for 1% fluctuation of electron density ($\Delta N/N = 10^{-2}$), increasing to 300 meters for 10% fluctuations and one kilometer for 100% fluctuations. One can make a self-consistent argument that a scatterer 100 meters off the line-of-sight having an electron density 1% below ambient

will reflect a ray to the receiver. The reflected amplitude will be significant if the reflecting surface is a reasonable fraction of a Fresnel zone, and this is achieved easily in one direction (the reflecting surface should be 50 meters normal to the path), but more difficult in the direction approximately along the path.

If the signals are to fade by the amounts observed, one can argue that the scatterer must be far enough off the line-of-sight that the phase difference between the direct and the scattered rays is large (the path difference is $\lambda/2$ at an offset of 170 meters, and λ at 320 meters) and this requires ($\Delta N/N$) to be about 5 and 10%, respectively.

The observed scintillations during disturbed periods up to 8 db (or more commonly in distrubed periods of 2 db) would require a direct ray and a scattered ray having an amplitude of 0.4 or (0.2) of the direct ray amplitude and an arbitrary phase. The combination would give a signal with phase variations up to 25° or (17°). In fact, a number of scatterers would probably contribute.

While the outline here is simplified, it suggests (1) that the observed scintillations in the tropics may be accounted for by refractive scattering, (2) that the uplink pilot beam may be subject tc refractive scattering and the question can only be answered with certainty by an experimental test.

Booker (1978) ascribes the localization of the observed scintillations to the tropics to a coincidence in the drift-velocity of the plasma and the phase-velocity of an acoustic gravity wave that leads to an amplification of the wave until it breaks. The condition for amplification, he believes, is satisfied in the tropics.

5.4 Application of Theory to the Uplink Pilot Signal

Ray theory. We first estimate the extra path imposed on a ray passing through an irregularity having an electron density N-ΔN compared with the ambient N. Adding statistically the effects of a number of irregularities traversed sequentially, we arrive at an extra length, or a phase difference between two rays, and find that the phase difference is about a degree.

The refractive index for a radio wave of angular frequency ω of an ionosphere of plasma frequency ω_N is

$$n = 1 - (\omega_N/\omega)^2$$

and $$\omega_N^2 \propto N .$$

Since the wave travels at a speed c/n through the medium, the extra path can be calculated by comparing the speed in the irregularity and the speed in the ambient medium. For the ray theory approach to the uplink problem, scales of the order of 10 meters are of interest since that is the separation in the ionosphere of two rays originating at the uplink transmitter and striking the edges of the SPS transmitting antenna. If one assumes the SPS beam may induce changes of 2% in the electron density then the change in index of refraction is 2×10^{-7} and the change in path length through a 10-meter irregularity 3×10^{-6} meters or 10^{-2} phase degrees at 2.45 GHz. If the ray travels through 200 km of ionosphere, encountering irregularities every 20 meters, then the number of independent samples is 10^4 and the statistical sum is 10^2 times the single irregularity extra path or about one degree. This should provide a phase jitter background of about a degree. At the higher frequency, 5.8 GHz, the phase difference is about one-fourth of a degree for these conditions.

Diffractive scattering. The inverse frequency squared scaling law of weak perturbation theory predicts very small scintillations at gigahertz frequencies using the observations at VHF or UHF as a reference point. The failure of diffractive scattering to account for the microwave scintillations observed at tropical ground stations and the weak microwave scintillations (a small fraction of a decibel) observed outside the tropics lead us to consider the next mechanism. Booker and Miller (1978), for example, develop expressions for the amplitude scintillations and the phase scintillations. The calculated mean-square phase fluctuations for $\Delta N/N = 1\%$ and $p = 4$ (see below) is 10^{-2} degrees squared through the ionosphere for conditions intended to match the large scintillations observed in the tropics.

To illustrate the nature of the problem of estimating the phase fluctuations, we quote expressions given by Booker and Miller for the phase fluctuations $\overline{(\Delta\varphi)^2}$ and the amplitude fluctuations $\overline{(\Delta A/A)^2}$

$$\overline{(\Delta\varphi)^2} = 4r_e^2\lambda^2 \int_0^{z_S} \overline{(\Delta N)^2}\ \mathrm{cosec}\psi\sec\chi \left\{\frac{1}{2\pi}\int_0^{\infty} \frac{1+\frac{1}{2}k^4T_F^4}{1+k^4T_F^4}\, S(k)dk\right\} dz$$

$$\overline{(\Delta A/A)^2} = 4r_e^2\lambda^2 \int_0^{z_S} \overline{(\Delta N)^2}\ \mathrm{cosec}\psi\sec\chi \left\{\frac{1}{2\pi}\int_0^{\infty} \frac{\frac{1}{2}k^4T_F^4}{1+k^4T_F^4}\, S(k)dk\right\} dz$$

where r_e is the classical electron radius (2.82×10^{-15} m),

$(\Delta N)^2$ is the mean square fluctuation of electron density,

z_S is the height of the satellite transmitting on a wavelength λ,

χ is the angle between the vertical and the ray from the satellite to the ground,

ψ is the angle between the propagation path and the earth's magnetic field at height z,

$S(k)$ is the spacial spectrum of fluctuations in the medium range of scales (i.e., not near the atmosphere scale height or the short scale cut-off taken to be the ionic gyroradius) which may be observed. It is assumed to have a dependence on the scale k^{-1} with an exponent p in the range 1 to 4, and

T_F is a Fresnel scale $\left(\frac{\lambda d}{2\sqrt{2}\ \pi}\right)^{\frac{1}{2}}$ at a distance d from the earth station.

The calculated results are plotted in Figure 5.4 (taken from Booker and Miller, 1978, Fig. 7) for phase and amplitude fluctuations per unit $\overline{(\Delta N/N)^2}$. For an electron density fluctuation $(\Delta N/N)$ of one percent, $\overline{(\Delta N/N)^2}$ is 10^{-4} and the ordinate is to be multiplied by 10^{-4}.

Refractive scattering. The calculation of the phase errors due to refractive scatter depends on the fractional changes in electron density $(\Delta N/N)$ that may be induced in the ionosphere by the microwave heating. In the previous section we argued that one percent fluctuations in electron density have a critical angle so close to 90 degrees that the displacement of the scatterer off the direct line-of-sight is too small to introduce anything but constructive interference of the direct and scattered rays. A ray scattered from an irregularity 100 meters off the direct path at a distance of 400 km from the receiver differs in phase from the direct ray by 30 degrees. If the two rays are equal in amplitude, the phase error of the combined signal is 15 degrees; if the scattered ray amplitude is a half, a quarter,

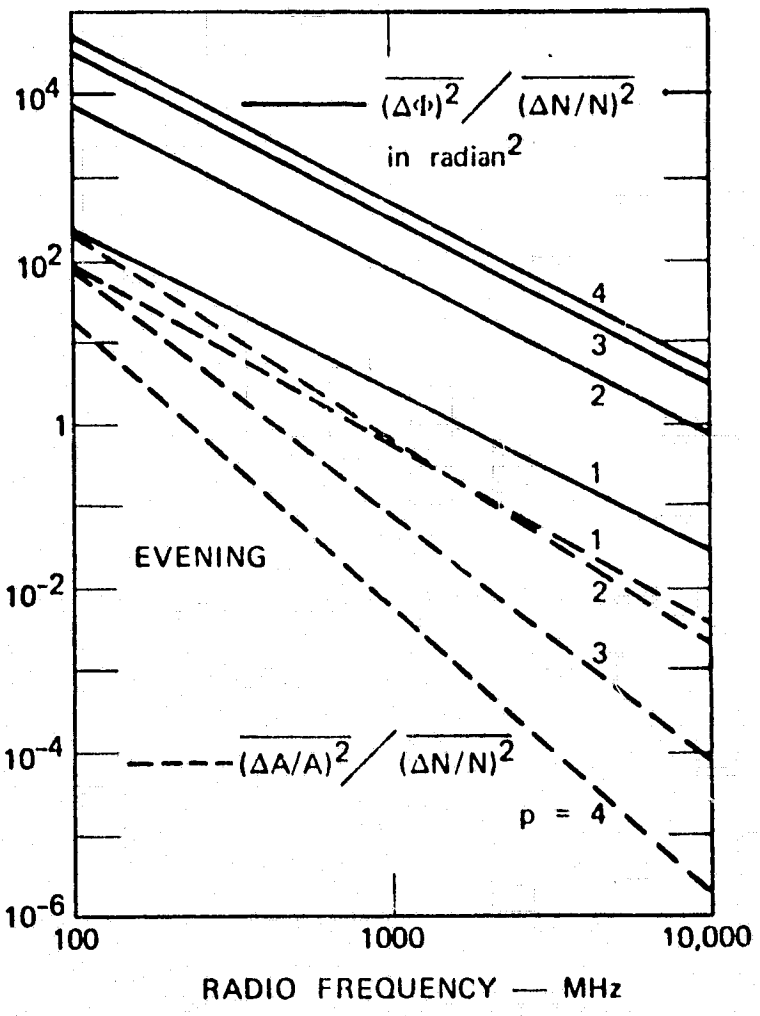

FIGURE 5.4

Frequency dependence of the mean square fluctuations of phase and of fractional amplitude, per unit $\overline{(\Delta N/N)^2}$, for the entire plasmasphere. Overhead stationary satellite at the magnetic equator. Evening.

a tenth, or a hundredth of the direct ray amplitude the phase error is 10 degrees, 6 degrees, 2.6 degrees or 0.3 degrees, respectively. Whereas what we have just called constructive interference is in fact the case and the amplitude scintillation is small; the phase error of the resultant could be as much as 15 degrees in the hypothetical case. This is probably an unlikely event since it is difficult to imagine that the amplitude could be very large.

The result is that the surprising observation of microwave scintillations in the tropics at certain times, unexplained so far except perhaps by Booker's breaking waves, raises a warning flag. If the SPS microwave beam can trigger some major instability in the ionosphere the uplink pilot beam may be in trouble.

5.5 Need for a Test

The present stages of development of the theories of ionospheric modification by intense radiowave heating and radiowave scintillation produced by irregularities make it impossible to predict with any confidence the effects of an ionosphere heated by the SPS microwave beam on the uplink pilot beam.

One could arrive at serious phasing problems with the uplink transmission by putting together the conditions: (1) the SPS microwave beam excites some instabilities in the ionospheric plasma or, at least, adds to the turbulent energy of the medium, and (2) the modified ionosphere behaves like the tropical ionosphere under disturbed conditions. Such a combination might cause the uplink beam to scintillate in a way that the proposed system could not tolerate. The likelihood of these conditions occurring cannot be estimated

reliably from theory and an experiment is required in which the scintillations of a microwave signal through a heated ionosphere are measured.

An extension of the experiment proposed by Duncan and Gordon (1977) would readily accommodate the additional requirements. The proposed experiment inserted radiowave energy into the ionosphere at the same rate and in the same volume as those of the SPS microwave beam. The radiowave used to heat the ionosphere is scaled to about 15 MHz where a reasonable and manageable amount of primary power will supply the required ionospheric input and the experiment is conducted with sufficient diagnostics to observe and understand the physical changes in the plasma. The extension of the experiment is to observe a microwave signal from a communication satellite in geosynchronous orbit through the modified ionosphere. The heating beam should be aimed at the geosynchronous orbit so that the incoming microwave signal propagates through the disturbed plasma at all heights of the ionosphere. The measurements on the ground would be the phase and amplitude scintillations and the spacial scales of the incoming microwave signal. Since communication satellites have transmissions near 1.5, 4 and 6 GHz, the SPS frequency can be bracketed. Full diagnostics should again be employed to map the physical changes in the plasma induced by the heating beam.

If the scintillation experiment were to be done at Arecibo, the heating beam would be directed about 20 degrees south of the zenith in order to aim it at the geosynchronous orbit. Such a tilt can be incorporated into the proposed experiment by reexamining the elements of the antenna array and by providing suitable phasing of the elements.

The results of the extension of the proposed experiment are (1) measured values of the phase fluctuations and the amplitude fluctuations, the former providing a direct

input to the question of the phase jitter at the satellite antenna, (2) the spacial scales or correlation distances of the phase and amplitude fluctuations which can be related to the scales in the ionosphere and then to the scales at the SPS, (3) these quantities can be measured when the ambient, natural ionospheric conditions are quiet and disturbed.

5.6 Reduction of the Phase Errors, if Large

There are at least two ways of reducing phase fluctuations imposed by a heated ionosphere that might be explored if needed. One has to do with the way the phase fluctuates with time and the reduction in the error is attempted by integrating the phase information over time. The second has to do with space and calls for moving the uplink transmitter from the center of the rectenna to a known position away from the antenna so that the uplink beam does not traverse the disturbed ionosphere. This approach requires that a built-in phase correction across the SPS transmitting antenna provides for the known displacement of the pilot source for the rectenna.

To evaluate the suggestion of integrating the phase information over time, one needs to consider the time rate of change (1) of the geosynchronous geometry, (2) of the flexing of the SPS structure supporting the transmitting antenna, (3) of any other time varying elements of the problem, and (4) of the phase fluctuations of the uplink signal. If the time rate of change of (4) is small compared to the others, then integrating the uplink phase information should help.

As an example, think of one aspect of the problem, the mechanical flexing of the support structure. As the

structure flexes one wishes to correct the phases of the individual modules of the SPS transmitting antenna so that the beam continues to be focused on the rectenna. If the structure flexes with periods of minutes, then the corrections must be applied at time intervals short compared with these periods to keep the beam properly formed and aimed. If the phase fluctuations have periods of seconds (Taur reports that most of the energy in the amplitude fluctuations is at periods less than 16 seconds for a disturbed tropical ionosphere), then the phase information derived at each module can be smoothed in time over periods 16 seconds or more, say a running average, and the smoothed phase information fed to the device controlling the phase of the output of the module. If the phase fluctuations have periods equal to or longer than the mechanical flexing period, then the smoothing does not help. In a similar way, the other geometrical, mechanical, electrical and other contributors to changing phase need to be examined and the fluctuation periods compared with the uplink fluctuation periods. The latter, of course, need to be determined by experiment, although the INTELSAT observations (Taur, 1977) in the disturbed tropics might be used as a starting point.

If the uplink pilot transmitter is moved away from the rectenna so that the path to the SPS avoids the disturbed ionosphere, then the uplink signal will be very stable except in the disturbed tropics which is not a factor for mid-latitude rectenna sites. The disturbed ionosphere includes the volume illuminated by the SPS microwave beam and some north-south elongation of the volume as the heated electrons travel along the earth's magnetic field lines. The elongation of the modified volume can be estimated theoretically from thermal time constants and mapped experimentally during the proposed tests.

If an uplink problem is shown to exist from a careful analysis of a well executed experiment, then the techniques for ameliorating the undesired effects should be applied to the observations to estimate the likely performance characteristics of the uplink pilot transmission.